PHYSICS AND CHEMISTRY OF SOLID STATE
V. 26, No.4 (2025) pp. 808-827
Section: Chemistry

DOI: 10.15330/pcss.26.4.808-827

Vasyl Stefanyk Carpathian National University

ФІЗИКА І ХІМІЯ ТВЕРДОГО ТІЛА
Т. 26, № 4 (2025) С. 808-827
Хімічні науки

UDK: 66.081.3:547.96]549.21

ISSN 1729-4428 (Print)
ISSN 2309-8589 (Online)

Iryna Prokipchuk[1], Ivan Myroniuk[1], Ihor Mykytyn[1], Hanna Vasylyeva[2]

Adsorption of proteins on carbon-based materials. Review

[1]*Department of Chemistry, Vasyl Stefanyk Carpathian National University, Ivano-Frankivsk, Ukraine, iryna.prokipchuk@pnu.edu.ua*
[2]*Department of Radiation Safety, Uzhhorod National University, Uzhhorod, Ukraine, h.v.vasylyeva@hotmail.com*

The adsorption of proteins on carbon-based materials is a complex and multifaceted process critical to applications in biotechnology, medicine, environmental science, and materials engineering. This review comprehensively examines the physicochemical mechanisms governing protein adsorption onto various carbon materials, including activated carbon, graphene, and graphene oxide. Emphasis is placed on the surface properties such as porosity, surface chemistry, wettability, and electric charge, as well as protein characteristics including size, structure, charge, and conformational dynamics. The influence of environmental factors – pH, ionic strength, and protein concentration – on adsorption behavior and protein layer formation is discussed. Special attention is given to the role of oxygen-containing functional groups on carbon surfaces and their impact on electrostatic and hydrogen bonding interactions. An overview of the analytical techniques used to study adsorption, including atomic force microscopy (AFM), circular dichroism (CD), isothermal titration calorimetry (ITC), quartz crystal microbalance (QCM), and spectroscopic methods is also provided. The review describes the role of protein adsorption onto carbon-based materials for their biomedical applications, namely, for implant biocompatibility and development of biosensors. Finally, a rapid growth in the number of works studying sorption on graphene oxide in recent years, as well as an increasing interest in its use for sensor development is highlighted.

Keywords: adsorption, graphene, graphene oxide, activated carbon, carbon adsorbents, theoretical models.

Received 24 August 2025; Accepted 30 October 2025.

Content

Abbreviations

AFM – atomic force microscopy
BSA – bovine serum albumin
CBMs – carbon-based materials
CD – circular dichroism
CNTs – carbon nanotubes
DLS – dynamic light scattering
DSC – differential scanning calorimetry
DWCNTs – double-walled carbon nanotubes
EGr – expanded graphite
FTIR – Fourier transform infrared spectroscopy
GnPs – graphene nanoplatelets
GO – graphene oxide
HSA – human serum albumin
ITC – isothermal titration calorimetry
MWCNTs – multi-walled carbon nanotubes
PALs – protein adsorption layers
PBS – phosphate-buffered saline
PFO – pseudo-first-order

pI – isoelectric point
pKa – negative logarithm of the acid dissociation constant
PSO – pseudo-second-order
PZC – point of zero charge
QCM – quartz crystal microbalance
rGO – reduced graphene oxide
RSA – Random Sequential Adsorption
SEM – scanning electron microscopy
TEM – transmission electron microscopy
TRP – trypsin
XPS – X-ray photoelectron spectroscopy
XRD – X-ray diffraction.

Introduction

The adsorption of proteins onto hydrophilic and hydrophobic solid surfaces is of critical importance in fields such as implantable device fabrication, biomimetic material design, bioelectronics, tissue engineering, protein crystallization, and implant biocompatibility. Protein adsorption is governed by various protein–protein and protein–surface interactions, including hydrophobic interactions, electrostatic forces, hydrogen bonding, and van der Waals interactions. Additionally, numerous factors influence the structure and stability of the adsorbed layer, such as protein concentration, ionic strength, temperature, and surface characteristics of the substrate [1].

This review focuses on protein sorption on carbon-based materials (CBMs). The most common type of them is naturally occurring three-dimensional (3D) carbon allotropes, graphite with sp^2 hybridized and diamond with sp^3 hybridized carbon networks [2]. A lot of recent research has been done on two-dimensional (2D) materials, graphene and graphene oxide (GO) [3-5]. A separate, relatively rare, case is one-dimensional (1D) carbon nanotubes (Fig. 1). Finally, many nanomaterials like fullerenes and carbon dots are considered zero-dimensional (0D) CBMs [6].

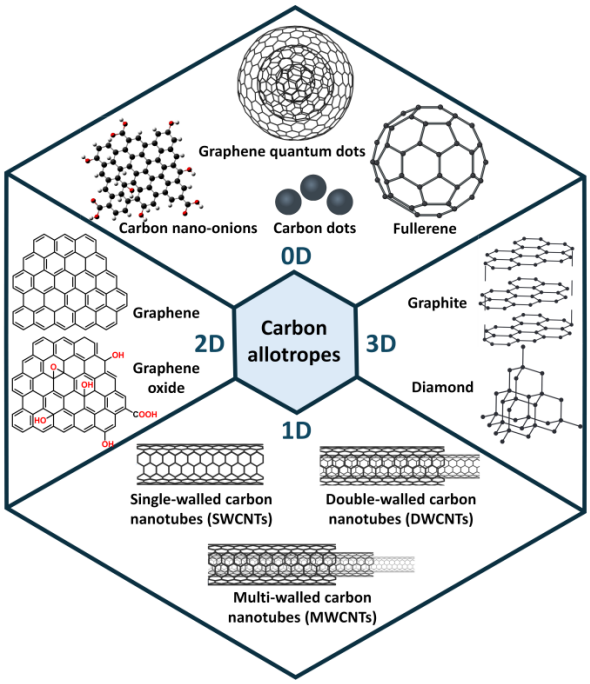

Fig. 1. Carbon allotropes classified as 0D, 1D, 2D, and 3D carbon nanostructures.

Most of the recent works in the field are focused on the application of CBMs for wound healing [7-9], drug delivery [10-12], tissue engineering [13-14], properties of GO and its applications for biosensor development [15-16]. However, available reviews are focused only on specific types of materials like GO and its composites or carbon nanotubes [17-19].

I. Proteins

1.1. Size of proteins. Difference between proteins and peptides

Proteins are high-molecular-weight amphoteric polyelectrolytes [20]. Both peptides and proteins are biological polymers composed of amino acids. Typically, species of 40 or fewer amino acids are referred to as peptides, whereas proteins contain 80 or more amino acids. Another way to distinguish between proteins and peptides is to account for their secondary structure. For proteins, secondary and tertiary structure are crucially important, while the properties of peptides usually do not depend on secondary structure at all. One more important difference between peptides and proteins relevant to the sorption properties is the accessibility of amino acids. All amino acids of peptides are generally accessible for interaction with the surface. Meanwhile, proteins, due to their ternary structure, have a lot of internal amino acids not exposed to the solvent or surface. It is worth noting that the distribution of exposed and internal amino acids in proteins is not random. Most of the hydrophobic amino acids are internal, while hydrophilic ones are predominantly exposed [21].

The size of the most common globular proteins is 3–5 nm. That corresponds to 150–350 amino acids. So, the contact area with the surface is about 10 nm^2. Most proteins in tissues and blood are 10–40 kDa and bear relatively low net charges, like 1–2 per every 10 amino acids of the sequence. The density of charges on the surface of proteins or peptides is low compared to that of the small organic molecules, which results in weaker electrostatic interactions and, consequently, lower adhesion [22].

Bovine serum albumin (BSA) is commonly used as a model protein in adsorption studies because of its structural stability, easy availability, and low cost. But what is important, BSA constitutes approximately 52–62 % of the total plasma protein content in blood, making it a relevant model protein. BSA is a globular protein with an approximate prolate spheroidal shape, measuring roughly 4 nm × 4 nm × 14 nm [23]. It has a molecular weight of 66 kDa [24] and consists of 583 amino acid residues arranged in a single polypeptide chain [25] and is characterized by considerable conformational flexibility.

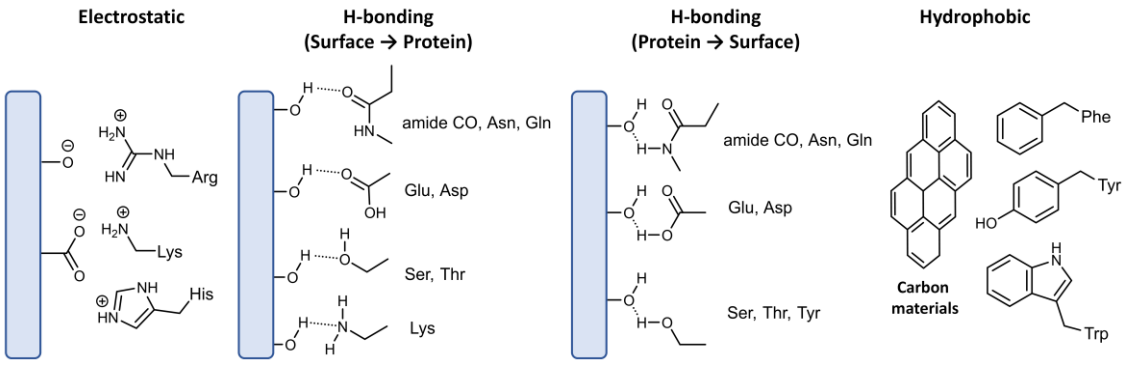

Fig. 2. Types of protein-surface interactions and amino acids typically involved in them.

Proteins are complex macromolecules composed of linear chains of amino acids and have several levels of structure. The primary structure refers to the specific sequence of amino acids in the polypeptide chain. Secondary structure arises from local conformations stabilized primarily by hydrogen bonding between the backbone amide and carbonyl groups, leading to regular motifs such as α-helices and β-sheets [26]. The tertiary structure represents the overall three-dimensional folding of a single polypeptide, driven by interactions among amino acid side chains, including hydrogen bonds, covalent disulfide bridges, hydrophobic effects, and electrostatic interactions. Quaternary structure describes the assembly and spatial arrangement of multiple polypeptide subunits into a functional complex, predominantly stabilized by non-covalent interactions, although disulfide bonds may also contribute. The native three-dimensional structure of monomeric proteins in most cases corresponds to the lowest energy conformation. However, protein folding is not a binary transition between native and unfolded states; instead, proteins can adopt numerous intermediate conformations corresponding to distinct low-energy states along the folding pathway [27]. Proteins with an α-helical conformation are more prone to changes in secondary structure when binding to a surface than proteins with a β or α/β conformation (see chapter 4 for detail discussion) [28].

1.2. Groups that determine adsorption. Hydrophobic, hydrophilic, acidic, and basic amino acids. Interaction with H-bond donors and acceptors

The protein sorption on the surface of CBMs can be mediated by electrostatic forces, hydrogen bond formation, hydrophobic interactions (Fig. 2), and other processes like π-stacking [29].

Typically, CBMs exhibit slight acidity due to the presence of carboxylic groups and phenol-like hydroxyl groups. Therefore, the primary type of electrostatic interactions occurs between anionic surfaces and cationic residues, such as arginine (Arg), lysine (Lys), and histidine (His). Hydrogen bonds can be either between the hydroxyl groups present at the surface and H-bond acceptors in the protein (amide CO, carboxyl groups in glutamic acid (Glu), aspartic acid (Asp), amino groups of basic residues, etc.) or between H-bond donors in the protein and H-bond acceptors, mainly oxygen, at the surface (Fig. 2). In this case, H-bond donors in protein can include the NH group of the peptide bond or the amide side chain of asparagine (Asn) and glutamine (Gln); the carboxyl group of Glu and Asp; the hydroxyl group of serine (Ser), threonine (Thr), and tyrosine (Tyr). Finally, there is a possibility of π-stacking between aromatic amino acids and the graphite-like surface of the sorbent [21].

1.3. Dependence of charge on pH

The isoelectric point (pI) of a protein is defined as the pH at which the net electric charge of the protein is zero. Accordingly, proteins are positively charged at a pH below their pI and negatively charged at a pH above their pI. In most cases, adsorption is more favorable at or near the protein's isoelectric point because of its lower solvation energy in less charged states. The isoelectric point is analogous to the point of zero charge (see chapter 3) but describes the protein.

The protein pI varies greatly from extremely acidic to highly alkaline values, ranging from about 4.0 to 12.0, depending on the amino acid composition, but for most proteins falls within the range of 4 to 7 [30]. Amino acid composition of a protein sequence primarily defines its pI, based on the combination of dissociation constant (pKa) values of the constituent amino acids. Among 20 common amino acids, two, aspartic acid (Asp) and glutamic acid (Glu), are negatively charged at physiological pH due to their carboxyl side chains, and three, lysine (Lys), arginine (Arg), and histidine (His), possess positively charged side chains [31].

1.4. Effect of ionic strength on protein conformation and solubility

An important factor to consider is the colloidal stability of proteins in buffer solutions, as buffers are widely employed to maintain proteins at a specific pH. Although the underlying mechanisms of protein stabilization by buffers are not fully elucidated, the most commonly accepted explanation involves the binding of buffer ions to oppositely charged amino acid residues on the protein surface. When salts are introduced into the buffer system, salt ions may compete with buffer ions for binding at these specific sites [32].

Ionic strength significantly influences protein behavior, particularly solubility, leading to phenomena such as "salting in" (enhanced solubility) or "salting out" (reduced solubility). A decrease in protein solubility with increasing ionic strength is often associated with changes in colloidal stability. At a given pH, a protein possesses a specific net charge, which typically promotes electrostatic

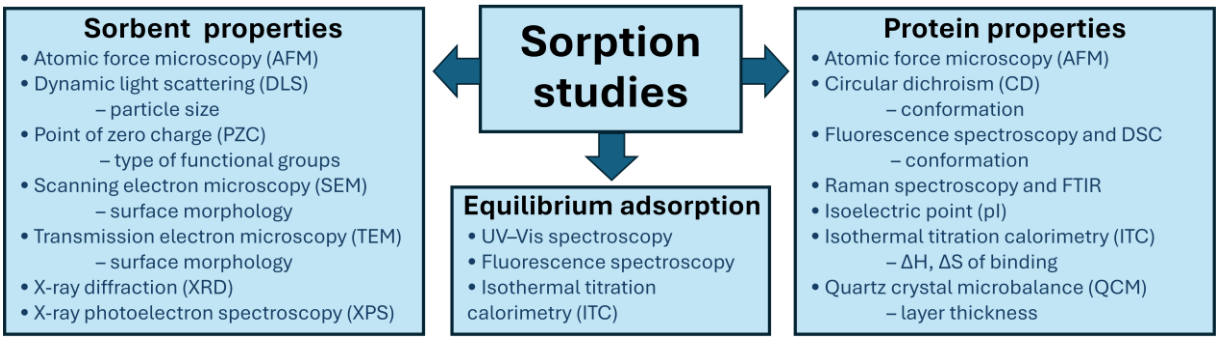

Fig. 3. Overview of methods used to study different aspects of protein sorption on CBMs.

repulsion between molecules and stabilizes the solution. However, as the ionic strength increases, electrostatic shielding reduces these repulsive forces, allowing attractive protein–protein interactions to prevail. This shift can promote aggregation and ultimately decrease solubility [33]. Physiological ionic strength corresponds to approximately 150 mM NaCl solution. So, buffers containing this concentration of salt are frequently used in studies of proteins.

II. Approaches to studying protein sorption

2.1. Techniques

The sorption of proteins on the CBMs is predominately studied using relatively stable globular proteins: bovine serum albumin (BSA) [34-36], human serum albumin (HSA) [37-39], lysozyme [40-42], trypsin (TRP) [43-45], bovine hemoglobin [46-48] and ubiquitin [49-51].

There are three main groups of methods used to study different aspects of protein sorption on CBMs (Fig. 3). The interaction of proteins with CBMs is investigated using UV–Vis spectroscopy [52-53], fluorescence spectroscopy [54-55], isothermal titration calorimetry (ITC) [56-57], atomic force microscopy (AFM) [58-59], circular dichroism (CD) [60-61], differential scanning calorimetry (DSC) [62-63], Fourier transform infrared spectroscopy (FTIR) [64-65], Raman spectroscopy [66-67], scanning electron microscopy (SEM) [68-69], X-ray diffraction (XRD) [5; 70], quartz crystal microbalance (QCM) [71] or ellipsometry [72].

The size and monodispersity of carbon particles can be determined by transmission electron microscopy (TEM) [73-74] and dynamic light scattering (DLS) [75-76]. The elemental composition of the CBMs is frequently analyzed using X-ray photoelectron spectroscopy (XPS) [77-78].

The most common and widely used method to study adsorption equilibrium and kinetics is the batch adsorption experiment [79-81]. Usually, it is carried out in Erlenmeyer flasks containing known initial concentrations of protein solutions and a fixed mass of adsorbent (Fig. 4). The suspensions are agitated using a magnetic stirrer flask shaker to ensure thorough mixing and contact between the protein molecules and the adsorbent surface. Following a specified contact time, aliquots of the suspension are transferred into centrifuge tubes and subjected to centrifugation to separate the solid and liquid phases. During this process, the adsorption equilibrium is assumed to be achieved. The supernatant is then carefully collected and placed into a cuvette, where the residual protein concentration is determined spectrophotometrically.

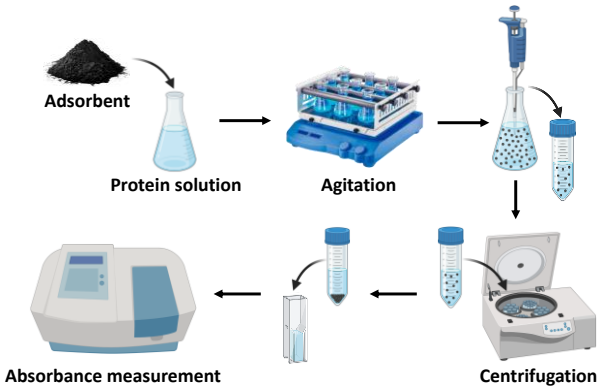

Fig. 4. Schematic representation of the adsorption experiments.

Using a buffer solution such as phosphate-buffered saline (PBS) is appropriate for protein dissolution because it maintains pH stability, enhances protein structural integrity, and mimics physiological conditions [82-84].

The adsorption capacity is calculated using Eq. (1) [85]:

$$q_e = \frac{(C_o - C_e) \cdot V}{m} \quad (1)$$

where q_e is the adsorption capacity (mg/g); C_o is the initial concentration of the adsorbate (mg/L); C_e is the equilibrium concentration of the adsorbate (mg/L); V is the total volume of solution (L); m is the mass of the adsorbent (g) [86]. In some cases, the concentration of the adsorbate and the adsorption capacity are expressed in molar (M) or millimole (mmol) units, for example, in works [87-88]. However, this practice is less common compared to the conventional use of mg/L and mg/g units, respectively.

The binding equilibrium can be studied using many other techniques. For example, DSC was used for investigating interactions between albumin and carbon material [37]. This method provides information on the amount of heat released or adsorbed during the process. DSC can be used to measure the calorimetric enthalpy of thermal denaturation of a protein both in solution and on a surface [89].

A very similar analytical technique, ITC, directly measures the heat exchanged during chemical or

biochemical interactions. It is suited for investigating the thermodynamics of ligand binding to biological macromolecules, as it enables comprehensive characterization of the interaction. ITC provides key parameters including the binding affinity (K_a or K_d), enthalpy change (ΔH), and entropy change (ΔS), offering valuable insight into the forces driving molecular recognition and complex formation [90]. It was used to study the adsorption of proteins on GO samples [49].

Among various techniques, protein adsorption kinetics can be effectively studied using QCM or ellipsometry. QCM quantifies minute mass changes on flat, fixed surfaces by monitoring frequency shifts of a quartz crystal. It is highly sensitive, but its application is limited by substrate compatibility and susceptibility to temperature and pressure fluctuations. On the other hand, ellipsometry is based on analyzing changes in polarized light upon reflection. It provides complementary information to QCM, allowing determination of optical properties and layer thicknesses with angstrom-level resolution. The method is non-destructive, suitable for real-time monitoring, and can also resolve spatial patterns of protein binding. However, a key limitation is the requirement for prior knowledge of the substrate's optical properties and the need for careful modeling to extract reliable data [72].

DLS provides information about the size distribution of carbon particles, for example, graphene or graphene oxide aggregates, as well as their zeta potential [91].

Molecular dynamics simulations are a distinct class of approaches to study protein sorption on CBMs. It can be used to interpret or explain the results of experiment-based techniques as well as to provide independent insights into the protein conformation changes upon binding. For example, molecular dynamics was employed to investigate the adsorption mechanism of BSA on a hydrophobic graphite surface [92]. It revealed that BSA undergoes significant spreading and partial unfolding upon free adsorption onto the hydrophobic graphite surface. The α-helical content, originally ~66 % in the native state, is reduced to approximately 25 % post-adsorption. Notably, these conformational changes are predominantly localized in the region of the protein in direct contact with the surface, while the upper portion largely retains its native secondary structure. Such information is complementary to experimental CD measurements that provide the overall α-helical content but cannot show the conformation of particular regions.

2.2. Models of equilibrium adsorption

The adsorption capacities of the materials are frequently studied under equilibrium conditions. The dependences of the amount of the adsorbed protein on its equilibrium concentration in solution at a constant temperature, so-called adsorption isotherms, provide an idea of the thermodynamic parameters and help to elucidate the interaction mechanism between the adsorbent and the adsorbate. These isotherms establish a relationship between the amount of adsorbate adsorbed per unit mass of adsorbent (q_e) and the equilibrium concentration of the adsorbate in solution (C_e), which serve as key indicators for characterizing the adsorption system. Liquid–solid adsorption isotherms are also employed to investigate the adsorption mechanism and to obtain information about the surface properties of the adsorbent and the nature of the adsorbate [93]. The equilibrium adsorption data is most frequently analyzed using the Langmuir and the Freundlich models. The Langmuir isotherm describes monolayer adsorption onto a surface with a finite number of identical, energetically equivalent adsorption sites, assuming no interaction between adsorbed molecules. The Freundlich isotherm is an empirical model that accounts for adsorption on heterogeneous surfaces with varying affinities and energies of adsorption sites (Fig. 5) [94]. These models are described by Eqs. (2) and (3), respectively [95].

$$q_e = \frac{q_{max} K_L C_e}{1 + K_L C_e} \tag{2}$$

$$q_e = K_f \times C_e^n \tag{3}$$

where q_{max} is the maximum adsorption value (mg/g); K_L is the Langmuir constant (L/mg); K_f is the Freundlich constant $\left(\frac{mg/g}{\left(\frac{mg}{L}\right)^n}\right)$; n is the Freundlich intensity parameter; C_e is the equilibrium concentration of the adsorbate (mg/L) [96].

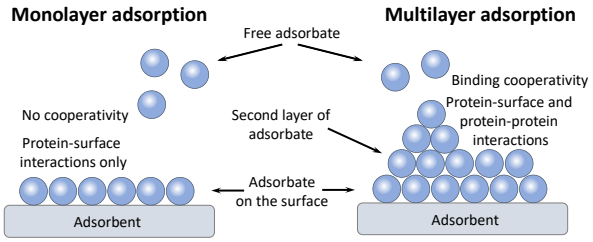

Fig. 5. Comparison of monolayer and multilayer adsorption models

The Langmuir and the Freundlich isotherms are frequently used in their linearized forms, Eqs. (4) and (5), respectively [97].

$$\frac{C_e}{q_e} = \frac{1}{q_{max} K_L} + \frac{C_e}{q_{max}} \tag{4}$$

$$\log q_e = \log K_F + \frac{1}{n} \log C_e \tag{5}$$

The key indicator of the Langmuir isotherm is the separation factor (R_L), which quantifies the favorability of an adsorption process (Eq. 6) [97].

$$R_L = \frac{1}{1 + K_L C_o} \tag{6}$$

The R_L values indicate the nature of the adsorption process: adsorption is unfavorable when $R_L > 1$, linear when $R_L = 1$, favorable when $0 < R_L < 1$, and irreversible when $R_L = 0$.

However, both the Langmuir and the Freundlich models exhibit significant limitations in accurately describing protein adsorption. Namely, the Langmuir model does not take into account that: (i) protein adsorption is often irreversible, (ii) the surface of the

material is rarely homogeneous, and (iii) processes such as protein unfolding and/or reorientation can occur. Unlike the Langmuir model, the Freundlich equation does not assume a uniform surface, making it more appropriate for systems in which proteins adsorb onto multiple nonequivalent binding sites. However, it assumes that saturation is never reached, but this assumption is unrealistic, particularly at high surface coverage [27].

Intermolecular interactions among adsorbed proteins dictate the maximum surface coverage and can lead to the formation of multilayer or bilayer structures. As a result of the complex electrostatics, protein adsorption often yields an irreversibly bound fraction – comprising molecules in direct contact with the surface – and a reversibly adsorbed fraction. This dual adsorption behavior frequently gives rise to non-classical adsorption isotherms, characterized by significant adsorption even at low bulk protein concentrations, and deviating markedly from ideal Langmuir-type models [98].

Several alternative models have been proposed to better account for both surface heterogeneity and the existence of a maximum adsorption capacity. Garrison Sposito introduced a modified version of the Freundlich equation that incorporates a saturation term to reflect maximum surface coverage [99]. Another approach, known as the Langmuir–Freundlich model, is derived from the Langmuir equation by adding an empirical heterogeneity factor. Despite their theoretical improvements, such models are still less commonly employed than the original Langmuir or the Freundlich isotherms, which remain widely used despite their underlying simplifications.

The Langmuir–Freundlich isotherm, also known as the Sips isotherm, is expressed by the following general equation [100]:

$$q_e = \frac{q_{MLF} K_{LF} C_e^{M_{LF}}}{1 + K_{LF} C_e^{M_{LF}}} \quad (7)$$

where q_{MLF} is the maximum adsorption capacity (mg/g); K_{LF} is the equilibrium constant; M_{LF} is the heterogeneity parameter ($0 < M_{LF} \leq 1$).

For homogeneous surfaces, the Random Sequential Adsorption (RSA) model was developed to address the limitations of the Langmuir isotherm. While RSA still assumes irreversible adsorption, it does not require an idealized, organized surface coverage, making it more realistic for systems where steric hindrance and spatial exclusion are significant factors [101]. The model is particularly applicable when proteins retain their native structure and orientation upon adsorption. However, more advanced models are required when protein unfolding, surface rearrangement, or desorption occurs. In such cases, multi-stage models are better suited to describe reversible adsorption processes and account for conformational changes during and after adsorption [102]. One such refinement is the rollover model, which accounts for protein reorientation on the surface, typically involving transitions from an end-on to a side-on configuration. This model has been applied, for instance, to describe the adsorption behavior of fibrinogen at high surface concentrations, where a secondary rearrangement stage occurs to minimize the interfacial free energy [103]. These models offer more nuanced insights into the dynamic and complex nature of protein–surface interactions, beyond the assumptions of classical isotherm models.

2.3. Sorption kinetics

The adsorption process involves the mass transfer of solute molecules from the liquid phase to the surface of the adsorbent. Kinetic models such as the pseudo-first-order (PFO) and pseudo-second-order (PSO) equations are widely used to investigate the adsorption kinetics of proteins onto CBMs [38].

The PFO equation, also known as the Lagergren first-order rate equation, is commonly used to describe adsorption processes in liquid-phase systems [104]. The differential form of the PFO kinetic equation is expressed as [105]:

$$\frac{dq_t}{dt} = k_1(q_e - q_t) \quad (8)$$

where q_e and q_t are the amount of protein adsorbed per unit mass of adsorbent at equilibrium and at time t, respectively (mg/mg); k_1 is the PFO rate constant (min^{-1}); t is the contact time between the adsorbent and adsorbate (min).

By integrating Eq. (8) and using the boundary conditions, $t = 0$ to $t = t$ and $q_t = 0$ to $q_t = q_t$, the integrated linear form is obtained and is represented in Eq. (9) [38]:

$$\log(q_e - q_t) = \log q_e - \frac{k_1}{2.303} t \quad (9)$$

The PSO kinetic model, also known as the Ho and McKay equation, is regarded as the most appropriate model for describing the adsorption of species in solution, particularly when chemisorption is the rate-limiting step [106]. The differential form of the PSO kinetic equation is expressed as [105]:

$$\frac{dq_t}{dt} = k_2(q_e - q_t)^2 \quad (10)$$

where k_2 is the PSO rate constant (min^{-1}).

By integrating Eq. (10) using the same boundary conditions as in Eq. (9), the following linear form of Eq. (10) is obtained [38]:

$$\frac{t}{q_t} = \frac{1}{k_2 q_e^2} + \frac{1}{q_e} \quad (11)$$

PFO and PSO models assume that the changes of adsorbate concentration during the process are negligible. Meanwhile, in diluted solutions, it is not correct. In cases where protein transport is solely governed by diffusion, the kinetics can be described by the Smoluchowski model [27]. It can be applied only when the protein concentration in solution is low and the surface coverage is close to zero. So, the number of occupied binding sites is negligible.

$$\Gamma(t) = 2C_b\sqrt{\frac{Dt}{\pi}} \quad (12)$$

where $\Gamma(t)$ denotes the interfacial concentration of the protein at time t; D is the diffusion coefficient; C_b represents the protein concentration in the bulk solution.

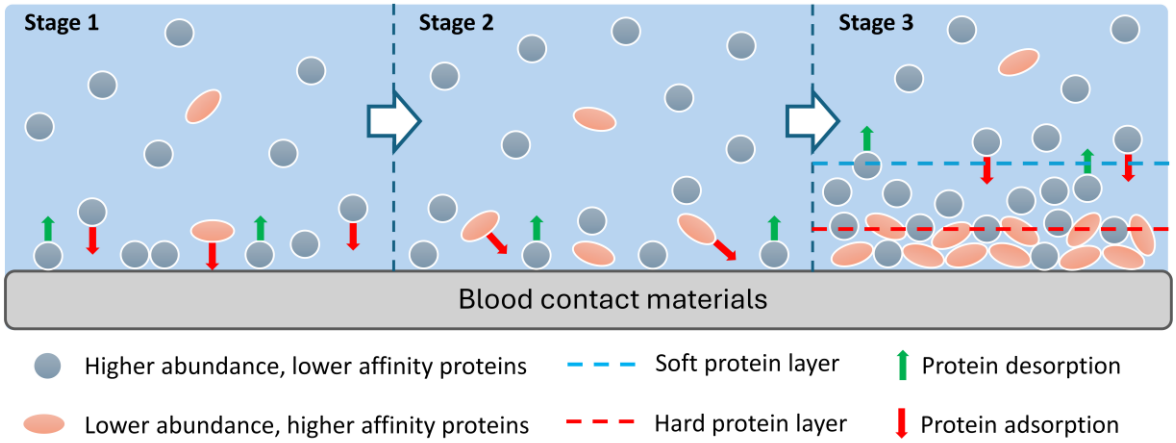

Fig. 6. Three key phases of protein sorption from a complex mixture with formation of protein adsorption layer(s) (based on the data from [107]).

In the more general case, protein adsorption onto solid surfaces typically proceeds through three sequential steps. The first involves the transport of protein molecules from the bulk solution to the solid–liquid interface, governed by diffusion and potentially enhanced by convective forces such as stirring or flow. The second step is the actual adsorption of the protein onto the surface. The final step concerns possible conformational rearrangements. When the transport step is slower than the interfacial adsorption reaction, it becomes the rate-limiting step, thereby controlling the overall adsorption kinetics [27].

The kinetics of protein sorption in real biological systems that contain multiple proteins is much more complex. The most practically important system is human blood, which contains thousands of proteins. When medical materials come into contact with blood, plasma proteins adsorb to their surface within seconds, but the stable equilibrated state is reached only in several hours. Plasma proteins vary in size and structure and can interact with a surface in diverse ways, leading to protein adsorption layers (PALs) of different composition, thickness, and stability. The changes are the composition of PALs over time proceed through three main stages (Fig. 6) [107].

First, plasma proteins present in high concentrations reach the surface and bind to it the earliest. HSA is one of the most abundant proteins in blood. However, in its natural conformation, it has a weak affinity for most CBMs and will quickly desorb, reaching equilibrium [107].

The second stage involves binding of plasma proteins, such as fibrinogen, which are present in a low concentration yet have high surface affinity [108-109]. Such proteins can continuously occupy the remaining space on the surface or directly replace proteins with weaker surface affinities, like HSA. With time, they constitute a stable substratum of PALs (Fig. 6, stage 2).

The third stage is similar to the second; plasma proteins can continue to adsorb to this substratum itself, subject to electrostatic, hydrophobic, and H-bonding interactions. Meanwhile, as the PAL thickens, the interaction of outer proteins with the surface weakens. In contrast, the role of protein-protein interactions and multilayer formation increases, leading to further stabilization of PAL composition, thickness, and structure [107]. In the case of nanoparticles, the layers are frequently called “corona” [110].

However, new reports suggest that upon contact with blood, serum albumin is likely to rapidly adsorb and spread across the graphite surface, forming a stable monolayer. This pre-adsorbed albumin layer can effectively occupy available binding sites, thereby limiting the subsequent adsorption of proteins such as fibrinogen and reducing the risk of blood clots on implant surfaces [92].

III. Carbon-based sorbents

Carbon is one of the most important natural elements. It has four valence electrons, which enable the mixing of atomic orbitals (2s and 2p) to form hybrid orbitals (sp, sp^2, and sp^3) [111]. The overlap of carbon atom hybrid orbitals results in the formation of strong σ-bonds, while any remaining unhybridized p atomic orbitals can participate in the formation of π-bonds. Unlike most other elements, which are typically found in molecular forms such as oxides, carbon is one of the few elements that occurs in its elemental form on Earth [112].

Carbon-based materials (Fig. 1) are characterized by high electrical conductivity, micro- and mesoporosity, and large specific surface [113]. They are widely used as adsorbents, particularly for air and water purification, filter production, as electrodes for lithium power sources, supercapacitors, fuel cells in electrochemistry, and as carriers of catalysts [114-115] and also in analytical chemistry [116]. CBMs of microporous structure can be prepared using the methods of thermal or thermochemical modification. Treatment of CBMs with H_2O or CO_2 at temperatures of 800–1100 °C leads to an increase in the pore volume in a carbon matrix, due to the interactions [117]. Porous carbon materials are primarily obtained through the pyrolysis (carbonization) of amorphous carbon at different temperatures, followed by thermal or chemical activation [118].

The surface chemistry of carbonaceous materials is fundamentally governed by the nature and distribution of acidic and basic surface sites. Acidic behavior is commonly associated with oxygen-containing surface complexes such as carboxylic acids, lactones, and

phenolic groups (Fig. 7). When dispersed in an aqueous medium, these functionalities can induce surface charge development, which depends on the pH [119]. Conversely, basicity is typically associated with functionalities including pyrones, chromenes, ethers, and carbonyl groups. Despite extensive investigation, the origin and nature of basic sites on carbon surfaces remain less well understood in comparison to their acidic counterparts, epoxides, and ethers [120].

The electronic behavior of these groups is governed by the hybridization state of the oxygen atoms involved. Oxygen atoms with sp^2 hybridization typically exhibit electron-withdrawing (acceptor) characteristics, whereas those with sp^3 hybridization act as electron-donating (donor) centers [121]. This distinction is critical for understanding the reactivity and stability of various oxygen-containing functional groups on carbon surfaces.

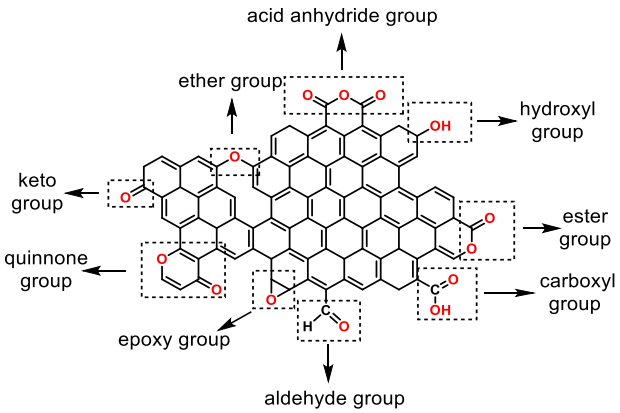

Fig. 7. Types of oxygen-containing functional groups on CBMs

Moreover, the spatial distribution of functional groups across the graphite sheets of carbon materials is non-uniform. Carbonyl and carboxyl groups are predominantly localized at the peripheries of graphite sheets (Fig. 7), where local reactivity is enhanced. In contrast, single-bonded groups like hydroxyl and epoxy functionalities are more broadly dispersed across the basal planes of the graphitic sheets [122]. The incorporation of double-bonded oxygen functionalities destroys the large-scale conjugated structure of the six-membered graphite ring, thereby increasing the energetic demands of such modifications. Consequently, these groups preferentially form at reactive edge sites, where the formation energy barrier is relatively lower [123]. The steric hindrance effect also influences the distribution position of oxygen-containing functional groups. The groups with elevated steric hindrance, such as carboxyl and carbonyl, due to their spatial demands, exhibit limited stability when embedded within the densely packed basal plane. These species tend to undergo structural rearrangement or conversion into less sterically hindered forms, such as hydroxyl groups, which are more easily accommodated within the graphitic lattice [122].

The adsorption properties of solid–liquid systems are significantly influenced by the presence of surface electric charges on both the adsorbent and the adsorbate. When carbon material is placed in contact with water, its surface undergoes ionization, which depends on the pKa values of its functional groups. Although the charged surface appears electrically neutral overall, it is surrounded by ions of the opposite charge [124]. The pH at which the net surface charge of carbon material is zero is known as the point of zero charge (PZC) (Fig. 8) [125]. At a pH higher than PZC, the surface bears a negative charge and more effectively adsorbs cations, while at a pH below PZC is cationic and has a higher affinity to anionic compounds. CBMs contain on their surface mostly hydroxylic and carboxylic groups that can be deprotonated but do not normally act as bases.

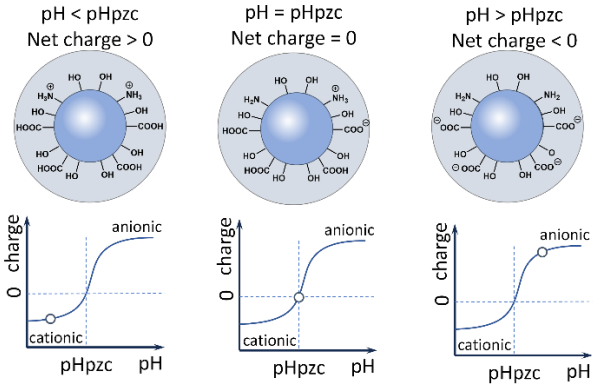

Fig. 8. Schematic representation of pHpzc of carbon materials.

Therefore, for most CBMs, PZC is in acidic pH. For example, PZC for GO is 2.00 – 4.3 [126-127] that is significantly lower than PZC for TiO_2 (5.35) [128-129]. Reported values for the PZC of activated carbon vary significantly across the literature, ranging from pH 2.2 to 8.4 [130-133].

The pHpzc of modified carbon materials can range widely, influenced by their specific preparation and modification processes, which can reach basic pH values. For example, GO–NH_2–Fe_3O_4 has 8.2 [134], nitrogen-doped activated carbon (AC5–600) has 9.7 [135], thermally treated activated carbon has 10.0 [133], GO–MgO has 10.5 [136].

3.1. Activated carbon

Activated carbon is a porous material with a high surface area that physically adsorbs molecules through noncovalent interactions [137]. It is produced from carbon-rich organic materials such as coconut shells, wood, coal, peat, and other sources [138]. Activated carbons are available in various forms and are typically classified based on the size and shape of their particles, which can be in the form of powder, pellets, or granules [139].

Carbon adsorbents possess a porous carbon structure that contains small amounts of heteroatoms such as oxygen and hydrogen. Some activated carbons also contain varying amounts of mineral matter (commonly referred to as ash content), which depends mainly on the nature and origin of the precursor material used in their synthesis. The porous structure is the main physical property that characterizes activated carbons. It is formed by pores of different sizes [140]. According to the recommendations of the IUPAC, porous materials are classified into three major categories (Fig. 9): micropores (<2 nm), mesopores (2–50 nm), and macropores

(> 50 nm) [141].

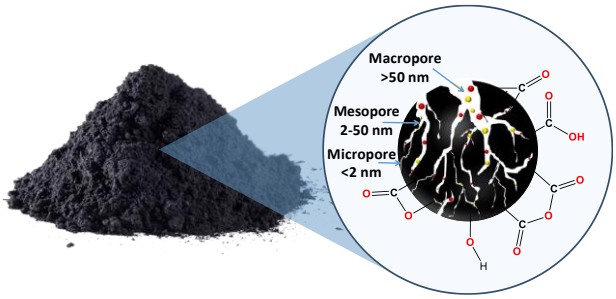

Fig. 9. Schematic presentation of pore structure and surface functional groups of activated carbon.

3.2. Graphene and graphene oxide

Graphene is a monolayer of carbon atoms arranged in a two-dimensional (2D) honeycomb lattice [142], characterized by sp^2 hybridization and a C–C bond length of approximately 0.142 nm [143]. It is the thinnest and one of the strongest known nanomaterials that exhibits a range of exceptional properties, including outstanding thermal and electrical conductivity, ultrafast electron mobility, and remarkable mechanical strength [144]. There are two main approaches to producing graphene – "top-down" and "bottom-up" [145]. The top-down method involves exfoliating graphite or its derivative, GO, to obtain graphene or its modified forms. The bottom-up method involves the formation of graphene through the condensation of carbon atoms during the thermal decomposition of a carbon-containing precursor [146].

One of the most studied derivatives of graphene is graphene oxide, an oxidized form of graphene functionalized with various oxygen-containing groups—primarily epoxides and hydroxyls on the basal plane, and carboxyl groups along the sheet edges (Fig. 10). In recent years, GO has garnered considerable attention due to its unique physicochemical properties. The abundance of oxygen-containing groups, particularly hydroxyl (–OH) and carboxyl (–COOH) groups, gives strong hydrophilicity to the material. As a result, GO readily disperses in water and a wide range of polar solvents, forming stable colloidal suspensions. The presence of reactive functional groups facilitates its versatile functionalization via covalent and noncovalent interactions with various molecules and biomolecules. Reduced graphene oxide (rGO) is a chemically modified form of GO, typically obtained through thermal, chemical, electrochemical, or other reduction techniques aimed at decreasing the content of oxygen-containing functional groups (Fig. 10). The partial restoration of the sp^2-conjugated carbon network during the reduction process imparts rGO with significantly enhanced electrical conductivity compared to GO. Despite the reduction, rGO retains a certain amount of residual oxygen functionalities, which contribute to its high specific surface area, improved electronic conductivity, and favorable mechanical properties [143]. The use of different reducing agents allows for controlled variation in the carbon-to-oxygen ratio, and overall chemical composition of reduced GO can be effectively tuned [147]. The sorption capacity of GO strongly, but non-linearly, depends on the oxidized state [148].

Graphene-based materials are for biotechnological and biomedical applications such as drug delivery, bioimaging, and biosensing [150]. GO modified with different substances is used as a sensor, including for vitamins [151], proteins in solution [152], and protein aggregation [153].

The adsorption kinetics of bovine serum BSA onto GO follow a PSO model, indicating a rapid process with high adsorption capacity [154]. A decrease in the melting temperature (Tm) and enthalpy change (ΔHm) suggests that BSA adsorbed on the GO surface becomes more susceptible to thermal denaturation. Notably, the presence of GO induces significant conformational alterations and activity changes of BSA. On the other hand, adsorption of BSA on the GO modifies its surface charge, decreasing GO aggregation [155]. Some works reported cytotoxicity of GO due to the formation of reactive oxygen species [156]. The fundamental step in the development of biosensors involves the physicochemical immobilization of biomolecules – particularly proteins – onto carbon-based electrodes. Nakanishi et al. [157] have highlighted the potential of protein adsorption onto nanocarbons, such as graphene, carbon nanotubes, and fullerenes, as an effective strategy for chemical functionalization of surfaces intended for nanosensor applications. Even on planar surfaces, the overall adsorption behavior typically results from the interplay of multiple interaction types. The surface chemistry and wettability are key factors determining the nature and strength of protein binding. In porous materials, additional effects such as size exclusion and confinement further influence adsorption behavior

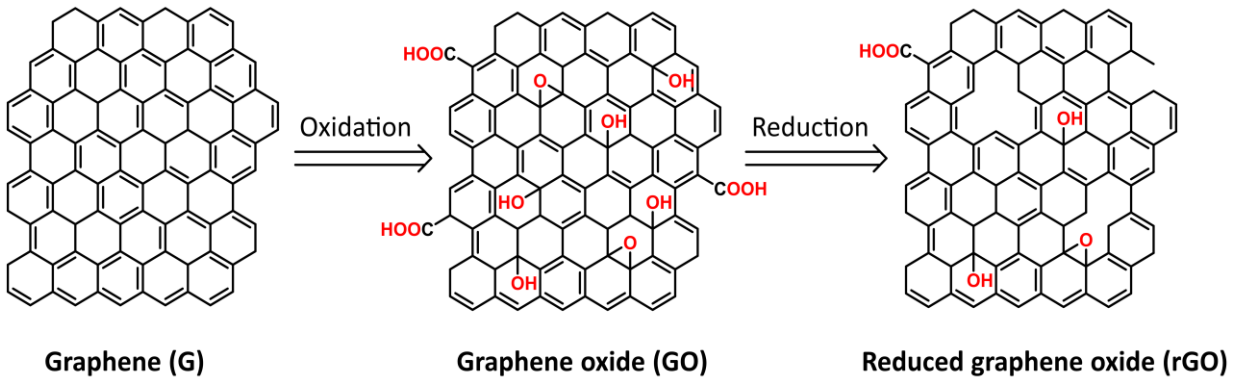

Fig. 10. Schematic representation of surface changes upon graphene oxidation and reduction that shows the formation of carboxy groups on the edges and hydroxy (epoxy) groups on the basal plane, as well as the presence of a significant amount of oxygen-containing groups in reduced graphene oxide (based on the data from [149]).

[158].

IV. Sorption on carbon-based materials

Protein adsorption at solid interfaces is a phenomenon of fundamental importance in numerous fields, including biotechnology, materials science, medicine, pharmaceutics, and food technology [159]. The adsorption capacity and selectivity are strongly influenced by the pore size of the adsorbent. For the efficient adsorption of large biomolecules such as proteins, the pore diameter should fall within the mesoporous range and be equal to or greater than the dimensions of the adsorbate molecule (3–10 nm for most proteins). An additional factor influencing protein adsorption is the electrostatic interaction between the adsorbate molecule and the surface of the adsorbent. Maximum adsorption is often observed near the pI of the protein; it can be due to suppression of electrostatic repulsion between protein molecules bound to the surface or between the protein and the adsorbent surface, as well as because of decreasing protein solubility (hydration energy). There are two main approaches to determine the threshold pore size required for protein adsorption. The first involves studying the adsorption behavior of proteins with varying molecular sizes. However, this method is less conclusive, as proteins differ not only in size but also in charge, shape, and hydrophobicity, making it difficult to isolate the effect of size alone. The second approach, more suitable for controlled investigations, involves studying protein adsorption on a series of adsorbents with well-defined and uniform pore sizes spanning the dimensions of the target protein. This method enables a more direct assessment of the pore size threshold necessary for effective adsorption [160].

Despite its relevance, the mechanisms governing protein adsorption and desorption remain incompletely understood due to the complexity and multifactorial nature of the interfacial interactions involved. These systems comprise multiple components (e.g., the solid surface, protein, and solvent), each with distinct physicochemical properties such as polarity and charge, highly dependent on environmental conditions, including pH, ionic strength, and temperature. Upon contact with a protein solution, the solid surface is initially wetted by solvent molecules. Proteins then diffuse toward the interface, displace the solvent, and adsorb onto the surface. Following initial adsorption, further processes such as conformational rearrangement, multilayer formation, or competitive displacement may occur, leading to the evolution of a complex adsorbed protein layer. Importantly, proteins can establish multiple contact points with the surface, resulting in a substantial Gibbs free energy of adsorption [161].

The surface properties and molecular characteristics of proteins influence the attachment time and the nature of interactions, often leading to conformational changes upon adsorption. A longer residence time generally promotes more pronounced conformational alterations, which in turn increase the strength of protein–surface interactions. At the molecular level, several parameters influence the extent and nature of protein adsorption [162]:

Protein size – Larger proteins provide more surface contact points, enhancing adsorption.

Surface charge of the protein – Adsorption is more favorable at or near the protein's isoelectric point.

Structural stability – Less stable proteins unfold more easily, exposing binding sites.

Unfolding rate – Rapidly unfolding proteins adsorb more quickly. Likewise, the characteristics of the solid surface also play a significant role in determining the adsorption behavior:

Surface topography – Greater surface area promotes more adsorption.

Surface composition – The chemical composition of the surface determines the nature of intermolecular interactions

Surface hydrophobicity – Generally, hydrophobic surfaces facilitate greater protein adsorption.

Surface heterogeneity – Variations in surface structure can create distinct domains, promoting diverse modes of protein binding.

Surface potential – This affects the distribution of counter-ions at the interface, which in turn modulates the adsorption process [163].

In aqueous systems, van der Waals forces, induced dipole interactions, dipole–dipole interactions, and hydrogen-bond donor–acceptor interactions contribute to the binding and accumulation of chemical compounds on various adsorbents. Among these, hydrogen bonding, π–π interactions, covalent and electrostatic interactions, and hydrophobic effects play significant roles in the adsorption process (Fig. 11) [93].

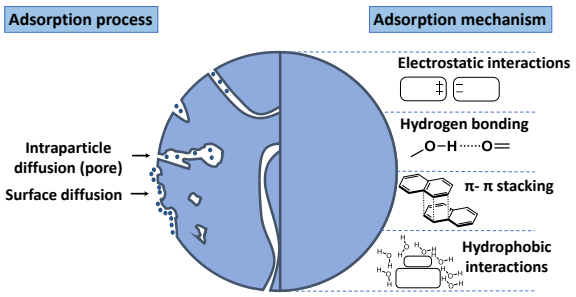

Fig. 11. Schematic representation of a possible adsorption mechanism of proteins on CBMs.

The adsorption of a protein on a surface can interfere with the adsorption of another protein, which is quite logical, since different proteins interact with the same functional groups on the surface of CBMs [164].

Proteins are inherently dynamic macromolecules that typically adopt complex, hierarchically organized conformations in aqueous environments. A delicate balance of non-covalent interactions, including hydrogen bonding, hydrophobic packing, van der Waals forces, and electrostatic interactions, maintains their native folded state. However, upon contact with solid interfaces—especially high-surface-area sorbents—this equilibrium can be changed [165]. This was shown on the example of BSA using CD spectroscopy [166]. The reason for the conformation change can be an increase in the surface contact area. These structural changes are often rapid and

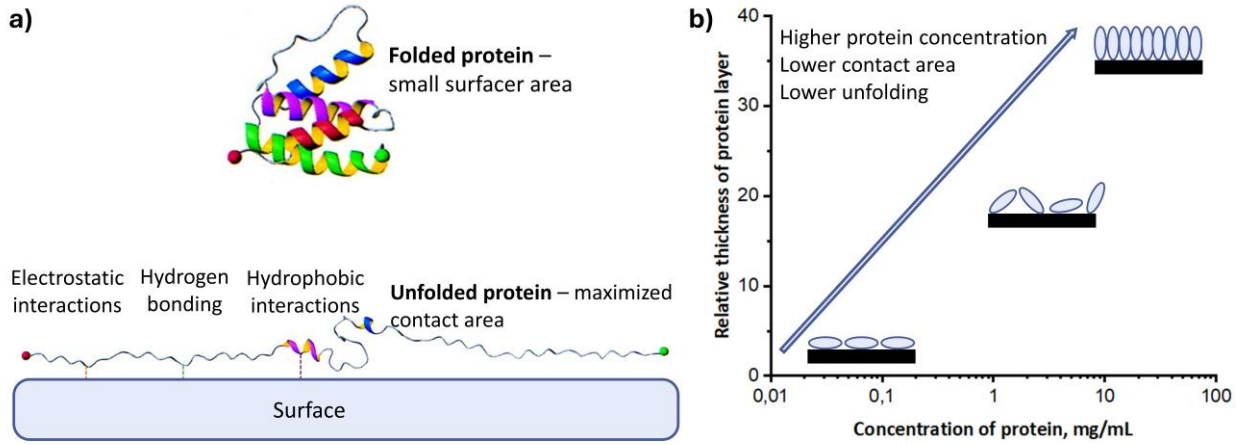

Fig. 12. a) Protein unfolding upon binding to the surface is governed by an increase in the interaction; b) changes of protein layer thickness depending on the equilibrium concentration of protein in solution show a change in protein conformation and binding mode.

exothermic, reflecting both enthalpic contributions from surface interactions and entropic gains from partial unfolding (Fig. 12a). For example, activated carbon surfaces, known for their hydrophobic character and π-electron-rich domains, can drive the partial denaturation of globular proteins such as BSA, lysozyme, and hemoglobin. Spectroscopic and calorimetric studies show that such events are often accompanied by the loss of α-helical content and the exposure of hydrophobic core residues [28].

The protein conformation on the surface and its binding mode depend on the concentration of the protein in solution, and the density of the surface (Fig. 12b). At low protein concentrations, the thin protein layer is formed, and adsorbed molecules primarily adopt a 'side-on' orientation. Upon adsorption, proteins may unfold or reorient from 'end-on' to 'side-on' to increase their surface footprint, thereby minimizing their free energy [167]. This spreading behavior is governed by the interplay between the protein's internal stability, protein–surface interaction strength, and inter-protein repulsion on the surface.

The degree of conformation change upon binding to the surface strongly depends on the nature of a protein. Even proteins with very similar structures can behave differently. For example, bovine and rat albumins have almost identical structure and the same α-helical content in solution (61–63 %). However, upon binding to the surface, BSA was unfolding much stronger, to 46 % α-helical content, compared to rat serum albumin (54 %) [168].

The results of Atsunori Sonoi's research group indicate that the protein adsorption orientation depends on the treatment concentration at the time of initial protein adsorption. When the surface coverage is low, such that proteins are not in contact with each other, orientation changes due to interactions among molecules are rare (Fig. 12b). Furthermore, researchers found that the initial orientation affected protein adsorption on the initially adsorbed layer. Highly crowded surface prevented the subsequent adsorption of proteins, inhibiting multilayer formation [169].

Different proteins exhibit varying degrees of conformational change upon adsorption. In 1990, T. Arai and W. Norde introduced the concept of "hard" and "soft" proteins [170], proposing that the conformational rigidity of proteins governs their adsorption behavior.

"Hard" proteins are characterized by high structural stability, and their adsorption is predominantly governed by electrostatic interactions. These proteins are sensitive to both the properties of the sorbent and their hydration shell. Adsorption of hard proteins onto hydrophilic surfaces occurs primarily when electrostatic interactions are favorable ($\Delta H < 0$). In such cases, electrostatic attraction is the main driving force, although the entropy change (ΔS), arising from charge redistribution during adsorption, may also contribute. On hydrophobic surfaces, adsorption may still occur even when ΔH is small due to a favorable entropic contribution ($T\Delta S > 0$) being the dominant driving force. In contrast to hard proteins, "soft" proteins exhibit low structural stability, and their adsorption involves additional driving forces associated with conformational changes. Unlike hard proteins, predicting the dominant thermodynamic contributions to the adsorption of soft proteins is more complex, as both enthalpic (ΔH) and entropic ($T\Delta S$) components must be considered [171]. Unfolding of the protein during adsorption increases entropy ($T\Delta S > 0$) and exposes internal residues, enabling the formation of additional interactions with the surface. This structural flexibility allows soft proteins to adsorb onto both hydrophobic and hydrophilic surfaces, regardless of whether electrostatic interactions are attractive or repulsive, in contrast to the behavior of hard proteins.

Regardless of the protein type, it tends to adopt a preferential conformation upon adsorption that minimizes its interfacial energy with the solid surface. Hard proteins largely retain their native structure during this process, making it meaningful to describe their orientation in terms of "side-on" or "end-on" configurations. The preferred orientation is primarily governed by the surface charge distribution and dipole moment of the protein, especially under electrostatic interaction conditions. The concept of "hard" and "soft" proteins is intrinsically linked to their ability to undergo structural modifications upon adsorption, which, from a thermodynamic perspective, is related to the standard Gibbs free energy of unfolding ($\Delta G°_{unf}$), governed primarily by intra-chain interactions.

This unfolding energy reflects the stability of the protein's secondary structure, which is determined mainly by its α-helix and β-sheet content. Significantly, $\Delta G°_{unf}$ is influenced not only by intrinsic structural factors but also by external parameters such as pH and ionic strength. Typically, hard proteins exhibit higher $\Delta G°_{unf}$ values (e.g., ~60 kJ·mol^{-1} for lysozyme), indicating greater conformational stability, whereas soft proteins have lower values (e.g. ~21 kJ·mol^{-1} for α-lactalbumin) [172]. Soft proteins tend to have a higher α-helix-to-β-sheet ratio and predominantly belong to the mainly α-class. In contrast, hard proteins are either mainly β or α/β-mixed with a layer sandwich architecture [27]. The ultimate case of soft proteins is intrinsically disordered proteins (IDPs). Among proteins frequently used for studies on carbon-based surfaces, lysozyme and streptavidin are classified as hard, while BSA, HSA, and myoglobin are considered soft.

A difference in sorption mechanism for one protein depending on the surface properties was shown by M. Seredych et al. [34]. They investigated the adsorption of BSA on thermally expanded graphite (EGr) and graphene nanoplatelets (GnPs). EGr was prepared by interacting graphite with a sulfuric/nitric acid mixture followed by thermal shock. For GnPs, the adsorption process was described by the Langmuir adsorption isotherm, indicative of monolayer adsorption on a homogeneous surface. The isotherm shows a clear tendency to plateau, suggesting the attainment of surface saturation. In contrast, no saturation was observed for EGr materials within the wide concentration range, implying multilayer adsorption or progressive occupation of heterogeneous binding sites (Table 1). In line with this observation, maximum protein adsorption capacities were remarkably high for EGr materials, which is suitable for usage as a carrier for high molecular weight biomolecules in biomedical applications. Meanwhile, GnP exhibits high adsorption efficiency at low BSA concentrations, suggesting a stronger affinity under dilute conditions. In both cases, the PSO kinetic model fitted the adsorption kinetic data (Table 1).

The mode of protein binding depends on pH and ionic strength. For example, under acidic conditions, HSA adsorption onto GO led to the formation of fluid, loosely packed protein layers, attributed to the extended conformation of the protein. Meanwhile, at neutral pH, the binding is denser, and increasing ionic strength enhanced the binding affinity between HSA and GO, resulting in the formation of more compact protein layers on the GO surface (Table 1). These results highlight the critical role of electrostatic interactions in governing HSA–GO interactions [37].

The adsorption of TRP onto the GO surface was examined and modeled at varying nanoparticle-to-protein

Table 1.

Isotherm parameters of the Langmuir and the Freundlich models for protein adsorption on CBMs

Adsorbent, adsorbate and conditions	**Maximum adsorption capacity (q_{max})**	**Isotherm constants (K_L, K_F, K_{LF}*)**	**Pseudo-second-order rate constant (k_2)**	**Ref.**
EGr, BSA in PBS	5.1 mg/g	K_F = 4.3 (mg/g)(L/mg)$^{1/n}$ K_{LF} = 0.0045 L/mg	0.39 g mg^{-1} min^{-1}	[34]
GnP, BSA in PBS	76.9 mg/g	K_F = 96.4 (mg/g)(L/mg)$^{1/n}$ K_{LF} = 1.75 · 10^{-5} L/mg	0.014 g mg^{-1} min^{-1}	
GO, HSA, 1 mM NaCl, pH 7.0	300 mg/g	K_F = 0.0032 (mg HSA)$^{1-n}$ L^n (mg GO)$^{-1}$	2.59 mg/mg·h	[37]
GO, HSA, 30 mM NaCl, pH 7.0	630 mg/g	K_F = 0.0451 (mg HSA)$^{1-n}$ L^n (mg GO)$^{-1}$	2.99 mg/mg·h	
GO, HSA, 150 mM NaCl, pH 7.0	660 mg/g	K_F = 0.2111 (mg HSA)$^{1-n}$ L^n (mg GO)$^{-1}$	35.71 mg/mg·h	
GO, TRP	100 mg/g	K_L = 0.083 L/mg K_F = 14.58 (mg·g^{-1})(L·mg^{-1})$^{1/n}$	–	[5]
GO, BSA in PBS	200.01 mg/g	–	0.00049 min^{-1}	[154]
MWCNTs, BSA, 40 °C, pH 5	127.2 mg/g	K_L = 0.0020 L/mg K_F = 1.20 mg/g	0.0071 min^{-1}**	[173]
MWCNTs, BSA, 40 °C, pH 4	139.5 mg/g	K_L = 0.0034 L/mg K_F = 1.88 mg/g	0.007 min^{-1}**	
MWCNT-ZrO_2, BSA, 40 °C, pH 4	273 mg/g	K_L = 0.0006 L/mg K_F = 0.20 mg/g	0.014 min^{-1}**	[174]
MWCNT-ZrO_2, BSA, 40 °C, pH 5	45 mg/g	K_L = 0.0071 L/mg K_F = 4.85 mg/g	0.018 min^{-1}**	
pristine MWCNTs in PBS	555.56 mg/g	K_L = 1.79 mL/mg K_F = 12.8 mg/g	–	[81]
treated MWCNTs in PBS	781.25 mg/g	K_L = 20.86 mL/mg K_F = 10.12 mg/g	–	
DWCNTs, BSA, 40 °C, pH 4	1221 mg/g	K_L = 0.00163 L/mg K_F = 137.0 mg/g	0.0083 min^{-1}**	[175]

*K_{LF} – Langmuir–Freundlich constant (L/mg)
**k_1 – pseudo-first-order rate constant (min^{-1})

ratios [5]. The adsorption was found to follow the Freundlich isotherm, characteristic of a heterogeneous system (Table 1). Langmuir model analysis revealed a maximum adsorption capacity of 100 mg/g. Extensive visualization of the TRP–GO interface was also performed for the 1:1 TRP–GO construct to elucidate the dynamic nature of the adsorption process. Samples collected at different adsorption time points were analyzed using SEM and AFM and revealed a gradual adsorption process, wherein initially local adsorption occurs slowly, leading to uniformity over the entire surface with time. Fluorescence and circular dichroism spectra of the 1:1 TRP–GO construct indicated that trypsin retains a high degree of its secondary β-sheet structure even after prolonged interaction with GO at a high protein-to-nanoparticle ratio. In this study GO was synthesized by using modified Hummer's method.

The Jian Cao's research group found that the adsorption of BSA onto GO follows a PSO model (Table 1), indicative of a rapid process with high adsorption capacity (200 mg/g). The adsorption process is driven by multiple noncovalent forces, including hydrophobic interactions, hydrogen bonding, van der Waals forces, and π–π stacking interactions, which collectively facilitate strong binding of BSA on the GO surface [154].

Adsorption BSA on multi-walled carbon nanotubes (MWCNTs) is characterized by a higher capacity than on GO. Equilibrium data were evaluated using Langmuir and Freundlich models, with maximum monolayer adsorption capacities at 40 °C determined to be 139.5 mg/g and 127.2 mg/g at pH 4 and 5, respectively (Table 1). Kinetic analyses revealed that the adsorption process conforms to the PFO model. Notably, the PFO rate constants at pH 4 and 5 decreased with increasing temperature, suggesting a reduction in the diffusion rate of BSA molecules across the external boundary layer, and favoring the sorption process. The diminished adsorption capacity observed at elevated pH values can be attributed to electrostatic repulsion between negatively charged BSA molecules and the MWCNTs surface [173]. In the other work of K. Bozgeyik & T. Kopac, the MWCNT–ZrO_2 composites were synthesized via a simple *in situ* chemical modification method. The adsorption equilibrium and kinetic data were analyzed using the Langmuir and the Freundlich models (Table 1). Adsorption kinetics was consistent with the PFO model, indicating diffusion-controlled adsorption [174].

Carbon nanotubes (CNTs) possess distinctive physical and chemical properties that make them attractive for biomedical applications [38]. The team of Saowapa T. Niyomthai studied the adsorption of BSA onto MWCNTs modified with H_2SO_4/HNO_3, and found a higher adsorption capacity of 771.87 mg/g compared to pristine MWCNTs (532.56 mg/g). Adsorption data for both materials were properly described by the Langmuir isotherm model (Table 1). The enhanced adsorption performance of the treated MWCNTs was attributed to a greater surface area and large amounts of oxygen-containing functional groups. Under desorption conditions, initial rapid release BSA was followed by a slower, sustained release phase, showing the potential of functionalized MWCNTs as carriers for prolonged drug release in biomedical applications [81].

The interactions and adsorption characteristics of BSA on double-walled carbon nanotubes (DWCNTs), produced by catalytic chemical vapor deposition, were examined. The adsorption kinetics and equilibrium processes were investigated through *in situ* UV–Vis spectroscopy. The maximum adsorption capacity was calculated as 1221 mg/g under optimal conditions, including (pH 4.0), adsorption time (420 min) and temperature (40 °C). The adsorption isotherm followed the Langmuir model, and the adsorption kinetics fitted the PFO (Table 1) [175].

Apart from commonly used CBMs, sorption is possible on modified diamond surfaces. For example, a research team led by M. Takai [176] compared the protein adsorption behaviors on rGO and boron-doped diamond surfaces using electrochemical impedance spectroscopy and found that sorption on the boron-doped diamond surface is much less dense. However, such studies are rare due to the high cost of diamonds.

Conclusions

Almost all research groups studying protein sorption on CBMs have used BSA and HSA, less often lysozyme and trypsin as model proteins. More than half of all works published during the last 5 years are devoted to GO sorption properties. The most widely used techniques to study the equilibrium of protein sorption on CBMs are UV–Vis spectroscopy, fluorescence spectroscopy, ellipsometry, and QCM. In contrast, a variety of additional techniques like AFM, DLS, DSC, FTIR, TEM, and CD are used to study protein conformation changes and their effect on the sorbent. To quantitatively describe the sorption process, the Langmuir–Freundlich and the Freundlich models are widely used.

Protein sorption occurs typically within 10–50 minutes. In most works, the pseudo-second order model is used for the description of sorption kinetics. Several more sophisticated models accounting for protein conformational changes were also proposed, but are almost not used in recent works. However, the concept of classifying proteins as hard or soft depending on their ability to undergo conformational changes is popular.

Most of the recent works investigating protein sorption on CBMs are focused on medicine-related applications: sensors, implants, tissue engineering, wound healing, and drug delivery.

Prokipchuk Iryna – M.Sc., leading specialist of the educational laboratory of the Chemistry Department;
Myroniuk Ivan – Doctor of Chemical Sciences, Professor and Head of the Chemistry Department;
Mykytyn Ihor – Candidate of Technical Sciences, Associate Professor of the Chemistry Department;
Vasylyeva Hanna – Candidate of Chemical Sciences, Head of the Department of Radiation Safety.

[1] S. Sarkar, S. Kundu, *Protein (BSA) adsorption on hydrophilic and hydrophobic surfaces,* Materials Today: Proceedings (2023); https://doi.org/10.1016/j.matpr.2023.04.200.
[2] A. Hirsch, *The era of carbon allotropes,* Nature Materials, 9(11), 868 (2010); https://doi.org/10.1038/nmat2885.
[3] J. Pérez-Piñeiro, et el., *Stability study of graphene oxide-bovine serum albumin dispersions,* Journal of Xenobiotics, 13(1), 90 (2023); https://doi.org/10.3390/jox13010008.
[4] P. Erwardt, K. Roszek, M. Wiśniewski, *Determination of graphene oxide adsorption space by lysozyme Uptake─Mechanistic studies*, The Journal of Physical Chemistry, 126(4), 928 (2022); https://doi.org/10.1021/acs.jpcb.1c08294.
[5] S. Kumari, et el., *Time-dependent study of graphene oxide-trypsin adsorption interface and visualization of nano-protein corona,* International Journal of Biological Macromolecules, 163, 2259 (2020); https://doi.org/10.1016/j.ijbiomac.2020.09.099.
[6] A. Yari-Ilkhchi, et el., *Graphene-based materials: an innovative approach for neural regeneration and spinal cord injury repair,* RSC Advances, 15(13), 9829 (2025); https://doi.org/10.1039/D4RA07976K.
[7] M. A. Rahman, et el., *Carbon-based nanomaterials: Carbon nanotubes, graphene, and fullerenes for the control of burn infections and wound healing,* Current Pharmaceutical Biotechnology, 23(12), 1483 (2022); https://doi.org/10.2174/1389201023666220309152340.
[8] M. A. Zarouki, et el., *Carbon nanostructures with antibacterial and wound healing activities: recent progress and challenges,* Journal of Materials Chemistry,13, 9745 (2025); https://doi.org/10.1039/D5TB00272A.
[9] Z. Sadat, et el., *A comprehensive review about applications of carbon-based nanostructures in wound healing: from antibacterial aspects to cell growth stimulation,* Biomaterials Science, 10(24), 6911 (2022); https://doi.org/10.1039/D2BM01308H.
[10] H. Singh, et el., *Carbon dots in drug delivery and therapeutic application,* Delivery Reviews, 224, 115644 (2025); https://doi.org/10.1016/j.addr.2025.115644.
[11] A. Kamboukos, N. Todorova, I. Yarovsky, *Exploring 2D graphene-based nanomaterials for biomedical applications: a theoretical modeling perspective,* Small Science, 5(6), 2400505 (2025); https://doi.org/10.1002/smsc.202400505.
[12] H. Dilenko, et el., *Graphene-based photodynamic therapy and overcoming cancer resistance mechanisms: A comprehensive review,* International Journal of Nanomedicine, 19, 5637 (2024); https://doi.org/10.2147/IJN.S461300.
[13] E. I. Biru, et el., *Graphene oxide–protein-based scaffolds for tissue engineering: Recent advances and applications,* Polymers, 14(5), 1032 (2022); https://doi.org/10.3390/polym14051032.
[14] R. Arambula-Maldonado, K. Mequanint, *Carbon-based electrically conductive materials for bone repair and regeneration,* Materials Advances, 3(13), 5186 (2022); https://doi.org/10.1039/D2MA00001F.
[15] J. Ye, Met el., *In silico bioactivity prediction of proteins interacting with graphene-based nanomaterials guides rational design of biosensor,* Talanta, 277, 126397 (2024); https://doi.org/10.1016/j.talanta.2024.126397.
[16] S. Shahriari, et el., Nanotechnology, *Graphene and graphene oxide as a support for biomolecules in the development of biosensors,* Science and Applications, 14, 197 (2021); https://doi.org/10.2147/NSA.S334487.
[17] K. Chaudhary, K. Kumar, P. Venkatesu, D. T. Masram, *Protein immobilization on graphene oxide or reduced graphene oxide surface and their applications: Influence over activity, structural and thermal stability of protein,* Advances in Colloid and Interface Science, 289, 102367 (2021); https://doi.org/10.1016/j.cis.2021.102367.
[18] D. Govindarajan, S. Saravanan, S. Sudhakar, S. Vimalraj, *Graphene: A multifaceted carbon-based material for bone tissue engineering applications,* ACS Omega, 9(1), 67 (2023); https://doi.org/10.1021/acsomega.3c07062.
[19] J. Meng, et el., *Interactions to plasma protein and application potentials of carbon nanotubes in blood-contacting medical devices,* Nano Research, 16(11), 12506 (2023); https://doi.org/10.1007/s12274-023-6170-4.
[20] D. A. Markelov, O. V. Nitsak, I. I. Gerashchenko, *Comparative study of the adsorption activity of medicinal sorbents,* Pharmaceutical Chemistry Journal, 42, 405 (2008); https://doi.org/10.1007/s11094-008-0138-2.
[21] A. Kessel, N. Ben-Tal Introduction to proteins: Structure, function, and motion, 2nd ed. (Chapman & Hall/CRC, Boca Raton, New York, 2018); https://doi.org/10.1201/9781315113876
[22] I. V. Prokipchuk, et el., *Fluorescence-based quantification of peptide adsorption on titanium dioxide,* Journal of Chemistry and Technologies, 31(3) (2023); https://doi.org/10.15421/jchemtech.v31i3.284204.
[23] T. Kopac, K. Bozgeyik, J. Yener, *Effect of pH and temperature on the adsorption of bovine serum albumin onto titanium dioxide,* Colloids and Surfaces A: Physicochemical and Engineering Aspects, 322(1–3), 19 (2008); https://doi.org/10.1016/j.colsurfa.2008.02.010.
[24] K. Baler, et el., *Electrostatic unfolding and interactions of albumin driven by pH changes: A molecular dynamics study,* The Journal of Physical Chemistry B 118(4), 921 (2014); https://doi.org/10.1021/jp409936v.
[25] P. S. Deulgaonkar, V. N. Lad, *Exploring the interfacial adsorption capability of bovine serum albumin*, Applied Surface Science Advances,11, 100276 (2022); https://doi.org/10.1016/j.apsadv.2022.100276.
[26] D. L. Nelson, M. M. Cox Lehninger Principles of Biochemistry, 8th ed. (W.H. Freeman, New York, 2021)
[27] D. Coglitore, J.-M. Janot, S. Balme, *Protein at liquid solid interfaces: Toward a new paradigm to change the approach to design hybrid protein/solid-state materials*, Advances in Colloid and Interface Science, 270, 278 (2019); https://doi.org/10.1016/j.cis.2019.07.004.
[28] P. Roach, D. Farrar, C. C. Perry, *Interpretation of protein adsorption: surface-induced conformational changes,* Journal of the American Chemical Society, 127(22), 8168 (2005); https://doi.org/10.1021/ja042898o.
[29] R. A. Hartvig, et el., *Protein adsorption at charged surfaces: The role of electrostatic interactions and interfacial charge regulation,* Langmuir, 27(6), 2634 (2011); https://doi.org/10.1021/la104720n.

[30] P. Novák, V. Havlíček, Protein Extraction and Precipitation, 2nd edn. (Elsevier, Amsterdam, 2016); https://doi.org/10.1016/B978-0-444-63688-1.00004-5.
[31] A. A. Tokmakov, A. Kurotani, K.-I. Sato, *Protein pI and intracellular localization,* Frontiers in Molecular Biosciences, 8, 775736 (2021); https://doi.org/10.3389/fmolb.2021.775736.
[32] P. Bharmoria, et el., *Do ionic liquids exhibit the required characteristics to dissolve, extract, stabilize, and purify proteins? Past-present-future assessment*, Chemical Reviews, 124(6), 3037 (2024); https://doi.org/10.1021/acs.chemrev.3c00551.
[33] S. J. Shire, Formulation of proteins and monoclonal antibodies (mAbs) (Elsevier, Amsterdam, 2015); https://doi.org/10.1016/B978-0-08-100296-4.00004-X.
[34] M. Seredych, L. Mikhalovska, S. Mikhalovsky, Y. Gogotsi, *Adsorption of bovine serum albumin on carbon-based materials,* C – Journal of Carbon Research, 4(1), 3 (2018); https://doi.org/10.3390/c4010003.
[35] B. Sun, Y. Zhang, W. Chen, K. Wang, L. Zhu, *Concentration dependent effects of bovine serum albumin on graphene oxide colloidal stability in aquatic environment*, Environmental Science & Technology, 52(13), 7212 (2018); https://doi.org/10.1021/acs.est.7b06218.
[36] P. Rubio‐Pereda, et el., *Albumin (BSA) adsorption onto graphite stepped surfaces,* The Journal of Chemical Physics, 146(21), 214704 (2017); https://doi.org/10.1063/1.4984037.
[37] X. Liu, C. Yan, K. L. Chen, *Adsorption of human serum albumin on graphene oxide: Implications for protein corona formation and conformation,* Environmental Science & Technology, 53(15), 8631 (2019); https://doi.org/10.1021/acs.est.8b03451.
[38] S. N. Barman, K. Kumari, A. S. Roy, *Adsorption of plasma protein human serum albumin on surface functionalized multi-walled carbon nanotubes: Insights into binding interactions and effects on protein fibrillation,* International Journal of Biological Macromolecules, 304, 140802 (2025); https://doi.org/10.1016/j.ijbiomac.2025.140802.
[39] H. Arzani, F. Ramezani, *Evaluation of the structure and conformation of albumin protein after interaction with graphene and graphene oxide,* Nano Biomedicine and Engineering, 14(4), 375 (2022); https://doi.org/10.5101/nbe.v14i4.p375-384.
[40] B. Li, et el., *Interaction of graphene oxide with lysozyme: Insights from conformational structure and surface charge investigations,* Spectrochimica Acta Part A: Molecular and Biomolecular Spectroscopy, 264, 120207 (2022); https://doi.org/10.1016/j.saa.2021.120207.
[41] S. Li, et el., *Strong and selective adsorption of lysozyme on graphene oxide,* ACS Applied Materials & Interfaces,6(8), 5704 (2014); https://doi.org/10.1021/am500254e.
[42] P. Du, J. Zhao, H. Mashayekhi, B. Xing, *Adsorption of bovine serum albumin and lysozyme on functionalized carbon nanotubes,* The Journal of Physical Chemistry C: Nanomaterials and Interfaces, 118(38), 22249 (2014); https://doi.org/10.1021/jp5044943.
[43] L. Li, et el., *Study of the interaction mechanism between GO/rGO and trypsin,* Journal of Hazardous Materials Advances, 3, 100011 (2021); https://doi.org/10.1016/j.hazadv.2021.100011.
[44] S. Huang, et el., *Investigations of conformational structure and enzymatic activity of trypsin after its binding interaction with graphene oxide,* Journal of Hazardous Materials, 392, 122285 (2020); https://doi.org/10.1016/j.jhazmat.2020.122285.
[45] H. Liu, et el., *The interaction of graphene oxide‐silver nanoparticles with trypsin: Insights from adsorption behaviors, conformational structure and enzymatic activity investigations,* Colloids and Surfaces B: Biointerfaces, 202, 111688 (2021); https://doi.org/10.1016/j.colsurfb.2021.111688.
[46] M. Chakraborty, et el., *Contrasting spectroscopic response of human hemoglobin in presence of graphene oxides and its reduced form: Comparative approach with carbon quantum dots,* Spectrochimica Acta Part A: Molecular and Biomolecular Spectroscopy, 247, 119079 (2021); https://doi.org/10.1016/j.saa.2020.119079.
[47] Y. Wang, et el., *Investigation on the conformational structure of hemoglobin on graphene oxide,* Materials Chemistry and Physics, 182, 272 (2016); https://doi.org/10.1016/j.matchemphys.2016.07.032.
[48] J. Tom, H. A. Andreas, *The influence of carbon-oxygen surface functional groups of carbon electrodes on the electrochemical reduction of hemoglobin,* Carbon,112, 230 (2017); https://doi.org/10.1016/j.carbon.2016.10.090.
[49] S. A. Malik, et el., *Modulation of protein–graphene oxide interactions with varying degrees of oxidation,* Nanoscale Advances, 2(5), 1904 (2020); https://doi.org/10.1039/C9NA00807A.
[50] G. Fang, et el., *Understanding the graphene quantum dots‐ubiquitin interaction by identifying the interaction sites,* Carbon, 121, 285 (2017); https://doi.org/10.1016/j.carbon.2017.05.096.
[51] S. Mondal, R. Thirupathi, L. P. Rao, H. S. Atreya, *Unraveling the dynamic nature of protein–graphene oxide interactions,* RSC Advances, 6(58), 52539 (2016); https://doi.org/10.1039/C6RA03759C.
[52] T. Kopac, K. Bozgeyik, E. Flahaut, *Adsorption and interactions of the bovine serum albumin‐double walled carbon nanotube system,* Journal of Molecular Liquids, 252, 1 (2018); https://doi.org/10.1016/j.molliq.2017.12.100.
[53] T. Kopac, K. Bozgeyik, *Equilibrium, kinetics, and thermodynamics of bovine serum albumin adsorption on single‐walled carbon nanotubes,* Chemical Engineering Communications, 203(9), 1198 (2016); https://doi.org/10.1080/00986445.2016.1160225.
[54] Z. Nan, C. Hao, X. Ye, Y. Feng, R. Sun, *Interaction of graphene oxide with bovine serum albumin: A fluorescence quenching study*, Spectrochimica Acta Part A: Molecular and Biomolecular Spectroscopy, 210, 348 (2019); https://doi.org/10.1016/j.saa.2018.11.028.

[55] X.-Q. Wei, et el., *Insight into the interaction of graphene oxide with serum proteins and the impact of the degree of reduction and concentration,* ACS Applied Materials & Interfaces,7(24), 13367 (2015); https://doi.org/10.1021/acsami.5b01874.
[56] V. Upadhyay, et el., *Isothermal titration calorimetry and surface plasmon resonance methods to probe protein-protein interactions,* Methods, 225, 52 (2024); https://doi.org/10.1016/j.ymeth.2024.03.007.
[57] Z. Ding, H. Ma, Y. Chen, *Interaction of graphene oxide with human serum albumin and its mechanism*, RSC Advances, 4(98), 55290 (2014); https://doi.org/10.1039/C4RA09613D.
[58] S. Kumar, S. H. Parekh, *Linking graphene-based material physicochemical properties with molecular adsorption, structure and cell fate,* Communications Chemistry, 3(1), 8 (2020); https://doi.org/10.1038/s42004-019-0254-9.
[59] S. Pandit, M. De, *Interaction of amino acids and graphene oxide: Trends in thermodynamic properties,* The Journal of Physical Chemistry C: Nanomaterials and Interfaces, 121(1), 600 (2017); https://doi.org/10.1021/acs.jpcc.6b11571.
[60] H. Pan, et el., *Nanoparticle-protein interactions: Spectroscopic probing of the adsorption of serum albumin to graphene oxide–gold nanocomplexes surfaces,* International Journal of Biological Macromolecules, 284, 138126 (2025); https://doi.org/10.1016/j.ijbiomac.2024.138126.
[61] X. Zhao, et el., *New insights into the behavior of bovine serum albumin adsorbed onto carbon nanotubes: Comprehensive spectroscopic studie,* The Journal of Physical Chemistry B, 114(16), 5625 (2010); https://doi.org/10.1021/jp100903x.
[62] S. G. Taneva, et el., *Insights into graphene oxide interaction with human serum albumin in isolated state and in blood plasma,* International Journal of Biological Macromolecules, 175, 19 (2021); https://doi.org/10.1016/j.ijbiomac.2021.01.151.
[63] C. M. Johnson, *Differential scanning calorimetry as a tool for protein folding and stability,* Archives of Biochemistry and Biophysics, 531(1–2), 100 (2013); https://doi.org/10.1016/j.abb.2012.09.008.
[64] N. Sharma, et el., *A review on exploring the impact of graphene oxide-based nanomaterials on structures and bioactivity of proteins,* Journal of Molecular Liquids 404, 124980 (2024); https://doi.org/10.1016/j.molliq.2024.124980.
[65] Y. Bai, et el., *Influence of graphene oxide and reduced graphene oxide on the activity and conformation of lysozyme,* Colloids and Surfaces B: Biointerfaces, 154, 96 (2017); https://doi.org/10.1016/j.colsurfb.2017.03.011.
[66] A. Khan, et el., *Mechanistic insight into the binding of graphene oxide with human serum albumin: Multispectroscopic and molecular docking approach,* Spectrochimica Acta Part A: Molecular and Biomolecular Spectroscopy, 256, 119750 (2021); https://doi.org/10.1016/j.saa.2021.119750.
[67] A. Wesełucha-Birczyńska, et el., *Raman studies of the interactions of fibrous carbon nanomaterials with albumin,* Spectrochimica Acta Part A: Molecular and Biomolecular Spectroscopy, 196, 262 (2018); https://doi.org/10.1016/j.saa.2018.02.027.
[68] D. Baimanov, R. Cai, C. Chen, *Understanding the chemical nature of nanoparticle-protein interactions,* Bioconjugate Chemistry, 30(7), 1923 (2019); https://doi.org/10.1021/acs.bioconjchem.9b00348.
[69] M. Šimšíková, *Interaction of graphene oxide with albumins: Effect of size, pH, and temperature,* Archives of Biochemistry and Biophysics, 593, 69 (2016); https://doi.org/10.1016/j.abb.2016.02.015.
[70] L. Stobinski, et el., *Graphene oxide and reduced graphene oxide studied by the XRD, TEM and electron spectroscopy methods,* Journal of Electron Spectroscopy and Related Phenomena, 195, 145 (2014); https://doi.org/10.1016/j.elspec.2014.07.003.
[71] H. Ishige, et el., *Evaluation of protein adsorption to diamond-like carbon (DLC) and fluorine-doped DLC films using the quartz crystal microbalance method,* Dental Materials Journal, 38(3), 424 (2019); https://doi.org/10.4012/dmj.2018-060.
[72] S. A. Bhakta, et el., *Protein adsorption onto nanomaterials for the development of biosensors and analytical devices: A review,* Analytica Chimica Acta, 872, 7 (2015); https://doi.org/10.1016/j.aca.2014.10.031.
[73] A. M. Sindi, *Applications of graphene oxide and reduced graphene oxide in advanced dental materials and therapies,* Journal of Taibah University Medical Sciences, 19(2), 403 (2024); https://doi.org/10.1016/j.jtumed.2024.02.002.
[74] S. Roy, et el., *Nanobio interface between proteins and 2D nanomaterials,* ACS Applied Materials & Interfaces, 15(30), 35753 (2023); https://doi.org/10.1021/acsami.3c04582.
[75] J. A. J. Housmans, G. Wu, J. Schymkowitz, F. Rousseau, *A guide to studying protein aggregation*, The FEBS Journal, 290(3), 554 (2023); https://doi.org/10.1111/febs.16312.
[76] M. Mahmoudi, et el., *Protein-nanoparticle interactions: Opportunities and challenges,* Chemical Reviews, 111(9), 5610 (2011); https://doi.org/10.1021/cr100440g.
[77] B. Sun, et el., *Impacts of photoaging on the interactions between graphene oxide and proteins: Mechanisms and biological effect,* Water Research, 216, 118371 (2022); https://doi.org/10.1016/j.watres.2022.118371.
[78] Hampitak, et el., *Protein interactions and conformations on graphene-based materials mapped using a quartz-crystal microbalance with dissipation monitoring (QCM-D),* Carbon, 165, 317 (2020); https://doi.org/10.1016/j.carbon.2020.04.093.
[79] S. Brandani, *Kinetics of liquid phase batch adsorption experiments*, Adsorption: Journal of the International Adsorption Society, 27(3), 353 (2021); https://doi.org/10.1007/s10450-020-00258-9.
[80] J. Kuchlyan, et el., *Spectroscopy and fluorescence lifetime imaging microscopy to probe the interaction of bovine serum albumin with graphene oxide*, Langmuir, 31(51), 13793 (2015); https://doi.org/10.1021/acs.langmuir.5b03648.
[81] S. T. Niyomthai, P. Pavasant, P. Supaphol, *Adsorption study of bovine serum albumin onto multiwalled carbon nanotubes,* Materials Today: Proceedings, 33, 1814 (2020); https://doi.org/10.1016/j.matpr.2020.05.060.

[82] P. Pavani, K. Kumar, A. Rani, P. Venkatesu, M.-J. Lee, *The influence of sodium phosphate buffer on the stability of various proteins: Insights into protein-buffer interactions,* Journal of Molecular Liquids, 331, 115753 (2021); https://doi.org/10.1016/j.molliq.2021.115753.
[83] T. Wei, S. Kaewtathip, K. Shing, *Buffer effect on protein adsorption at liquid/solid interface,* The Journal of Physical Chemistry C: Nanomaterials and Interfaces, 113(6), 2053 (2009); https://doi.org/10.1021/jp806586n.
[84] Y. L. Jeyachandran, E. Mielczarski, B. Rai, J. A. Mielczarski, *Quantitative and qualitative evaluation of adsorption/desorption of bovine serum albumin on hydrophilic and hydrophobic surfaces,* Langmuir, 25(19), 11614 (2009); https://doi.org/10.1021/la901453a.
[85] I. Mironyuk, et el., , *Adsorption of Sr(II) cations onto titanium dioxide, doped with Boron atoms,* Physics and Chemistry of Solid State, 24(1), 114 (2023); https://doi.org/10.15330/pcss.24.1.114-125.
[86] H. Vasylyeva, et el., *A new way to ensure selective zirconium ion adsorption,* Radiochimica Acta, 109(12), 877 (2021); https://doi.org/10.1515/ract-2021-1083.
[87] A. E. Orduz, G. P. Zanini, M. J. Avena, *Adsorption isotherm and removal efficiency. How are they related?* Journal of Chemical Education, 101(11), 5003 (2024); https://doi.org/10.1021/acs.jchemed.4c00828.
[88] A. Świątkowski, E. Kuśmierek, K. Kuśmierek, S. Błażewicz, *The influence of thermal treatment of activated carbon on its electrochemical, corrosion, and adsorption characteristics,* Molecules, 29(20), 4930 (2024); https://doi.org/10.3390/molecules29204930.
[89] L. Feng, J. D. Andrade, *Protein adsorption on low-temperature isotropic carbon: I. Protein conformational change probed by differential scanning calorimetry,* Journal of Biomedical Materials Research, 28(6) 735 (1994); https://doi.org/10.1002/jbm.820280611.
[90] C. J. Murciano-Calles, et el., *Isothermal titration calorimetry: Thermodynamic analysis of the binding thermograms of molecular recognition events by using equilibrium models. In Applications of Calorimetry in a Wide Context - Differential Scanning Calorimetry*, Isothermal Titration Calorimetry and Microcalorimetry (InTech, 2013); https://doi.org/10.5772/53311.
[91] A. M. Onaş, et el., *Novel bovine serum albumin protein backbone reassembly study: Strongly twisted β-sheet structure promotion upon interaction with GO-PAMAM,* Polymers, 12(11), 2603 (2020); https://doi.org/10.3390/polym12112603.
[92] C. Mücksch, H. M. Urbassek, Langmuir, *Molecular dynamics simulation of free and forced BSA adsorption on a hydrophobic graphite surface,* The ACS Journal of Surfaces and Colloids, 27(21), 12938 (2011); https://doi.org/10.1021/la201972f.
[93] M. M. Sabzehmeidani, et el, *Carbon based materials: a review of adsorbents for inorganic and organic compounds,* Materials Advances, 2(2), 598 (2021); https://doi.org/10.1039/D0MA00087F.
[94] H. Vasylyeva, et el., *Equilibrium studies of yttrium adsorption from aqueous solutions by titanium dioxide,* Applied Radiation and Isotopes, 168, 109473 (2021); https://doi.org/10.1016/j.apradiso.2020.109473
[95] I. Mironyuk, et el., *Adsorption of yttrium by the sodium-modified titanium dioxide: Kinetic, equilibrium studies and investigation of Na-TiO_2 radiation resistance,* Inorganic Chemistry Communications, 156, 111289 (2023); https://doi.org/10.1016/j.inoche.2023.111289.
[96] H. Vasylyeva, et el., *Application of titanium dioxide for zirconium ions adsorption and separation from a multicomponent mixture,* Physics and Chemistry of Solid State, 22(3), 460 (2021); https://doi.org/10.15330/pcss.22.3.460-469.
[97] N. Ayawei, A. N. Ebelegi, D. Wankasi, *Modelling and interpretation of adsorption isotherms,* Journal of Chemistry, 2017, 3039817 (2017); https://doi.org/10.1155/2017/3039817.
[98] Z. Adamczyk, *Protein adsorption: A quest for a universal mechanism,* Current Opinion in Colloid & Interface Science, 41, 50 (2019); https://doi.org/10.1016/j.cocis.2018.11.004.
[99] G. Sposito, *Derivation of the Freundlich equation for ion exchange reactions in soils,* Soil Science Society of America Journal, 44(3), 652 (1980); https://doi.org/10.2136/sssaj1980.03615995004400030045x.
[100] P. Pourhakkak, Aet el., Fundamentals of adsorption technology. In Interface Science and Technology (Elsevier, 2021); https://doi.org/10.1016/B978-0-12-818805-7.00001-1
[101] P. Schaaf, J.-C. Voegel, B. Senger, *From random sequential adsorption to ballistic deposition: A general view of irreversible deposition processes,* The Journal of Physical Chemistry B, 104(10), 2204 (2000); https://doi.org/10.1021/jp9933065.
[102] M. Rabe, D. Verdes, S. Seeger, U*nderstanding protein adsorption phenomena at solid surfaces,* Advances in Colloid and Interface Science, 162(1–2), 87 (2011); https://doi.org/10.1016/j.cis.2010.12.007.
[103] P. Roach, D. Farrar, C. C. Perry, *Surface tailoring for controlled protein adsorption: effect of topography at the nanometer scale and chemistry,* Journal of the American Chemical Society, 128(12), 3939 (2006); https://doi.org/10.1021/ja056278e.
[104] W. Plazinski, W. Rudzinski, A. Plazinska, *Theoretical models of sorption kinetics including a surface reaction mechanism: a review,* Advances in Colloid and Interface Science, 152(1–2), 2 (2009); https://doi.org/10.1016/j.cis.2009.07.009.
[105] J. Wang, X. Guo, *Adsorption kinetic models: Physical meanings, applications, and solving methods,* Journal of Hazardous Materials, 390, 122156 (2020); https://doi.org/10.1016/j.jhazmat.2020.122156.
[106] J. P. Vareda, *On validity, physical meaning, mechanism insights and regression of adsorption kinetic models* Journal of Molecular Liquids, 376, 121416 (2023); https://doi.org/10.1016/j.molliq.2023.121416.
[107] X. Chen, J. Chen, N. Huang, *The structure, formation, and effect of plasma protein layer on the blood contact materials: A review*, Biosurface and Biotribology, 8(1), 1 (2022); https://doi.org/10.1049/bsb2.12029.

[108] L.-C. Xu, J. W. Bauer, C. A. Siedlecki, *Proteins, platelets, and blood coagulation at biomaterial interfaces* Colloids and Surfaces B: Biointerfaces, 124, 49 (2014); https://doi.org/10.1016/j.colsurfb.2014.09.040.
[109] K. S. Lavery, et el., *Anti-thrombotic technologies for medical devices* Advanced Drug Delivery Reviews, 112, 2 (2017); https://doi.org/10.1016/j.addr.2016.07.008.
[110] F. Fu, et el., *In situ characterization techniques of protein corona around nanomaterials,* Chemical Society Reviews, 53(22), 10827 (2024); https://doi.org/10.1039/D4CS00507D.
[111] Q.-L. Yan, et el., *Highly energetic compositions based on functionalized carbon nanomaterials,* Nanoscale, 8(9), 4799 (2016); https://doi.org/10.1039/C5NR07855E.
[112] E. Picheau, et el., *An introduction to the combustion of carbon materials*, Chemistry – A European Journal, 28(54), e202200117 (2022); https://doi.org/10.1002/chem.202200117.
[113] V. I. Mandzyuk, et el., *Structure and electrochemical properties of saccharide-derived porous carbon materials,* Journal of Nano- and Electronic Physics, 10(2), 02018 (2018); https://doi.org/10.21272/jnep.10(2).02018.
[114] V. I. Mandzyuk, I. F. Mironyuk, Y. O. Kulyk, *Structure-morphological and electroconductive properties of carbon materials based on saccharose and citric acid,* Physics and Chemistry of Solid State, 21(3), 486 (2020); https://doi.org/10.15330/pcss.21.3.486-491.
[115] V. I. Mandzyuk, et el., *Impedance spectroscopy of capacitor systems based on saccharide-derived porous carbon materials,* Physics and Chemistry of Solid State, 22(4), 711 (2021); https://doi.org/10.15330/pcss.22.4.711-716.
[116] H. V. Vasylyeva, et el., *Radiation-induced processes in commercially available samples of activated carbon under the influence of gamma- and beta-radioactivity,* Journal of Nano- and Electronic Physics, 17(3), 03028 (2025); https://doi.org/10.21272/jnep.17(3).03028.
[117] V. I. Mandzyuk, et el., *Template synthesis of mesoporous carbon materials for electrochemical capacitors,* Surface Engineering and Applied Electrochemistry, 56(1), 93 (2020); https://doi.org/10.3103/s1068375520010123.
[118] N. Y. Ivanichok, et el., *Porous structure of carbon materials obtained from the shell of walnuts,* Physics and Chemistry of Solid State, 23(1), 172 (2022); https://doi.org/10.15330/pcss.23.1.172-178.
[119] J. A. Menéndez, *Electrical charge distribution on carbon surfaces as a function of the pH and point of zero charge. An approximate solution,* Research & Development in Material Science, 8(5) (2018); https://doi.org/10.31031/RDMS.2018.08.000697.
[120] M.V.Lopez-Ramon, et el., *On the characterization of acidic and basic surface sites on carbons by various techniques,* Carbon, 37(8), 1215 (1999); https://doi.org/10.1016/S0008-6223(98)00317-0.
[121] G. Ghanashyam, H. K. Jeong, *Plasma treated carbon nanofiber for flexible supercapacitors,* Journal of Energy Storage, 40, 102806 (2021); https://doi.org/10.1016/j.est.2021.102806.
[122] C. Qiu, L. Jiang, Y. Gao, L. Sheng, *Effects of oxygen-containing functional groups on carbon materials in supercapacitors: A review,* Materials & Design, 230, 111952 (2023); https://doi.org/10.1016/j.matdes.2023.111952.
[123] H. P. Boehm, *Surface oxides on carbon and their analysis: a critical assessment,* Carbon, 40(2), 145 (2002); https://doi.org/10.1016/S0008-6223(01)00165-8.
[124] V. Bernal, L. Giraldo, J.C. Moreno-Piraján, *Physicochemical properties of activated carbon: Their effect on the adsorption of pharmaceutical compounds and adsorbate–adsorbent interactions,* C – Journal of Carbon Research, 4(4), 62 (2018); https://doi.org/10.3390/c4040062.
[125] M. Kosmulski, *The pH dependent surface charging and points of zero charge. X. Update,* Advances in Colloid and Interface Science, 319, 102973 (2023); https://doi.org/10.1016/j.cis.2023.102973.
[126] L. C. de Almeida, et el., *Novel nanobiocatalyst constituted by lipase from Burkholderia cepacia immobilized on graphene oxide derived from grape seed biochar,* C – Journal of Carbon Research, 9(1), 12 (2023); https://doi.org/10.3390/c9010012.
[127] S. E. Bourachdi, et el., *Enhancing graphene oxide production and its efficacy in adsorbing crystal Violet: An in-depth study of thermodynamics, kinetics, and DFT analysis,* International Journal of Chemical Engineering, 2024 (2024); https://doi.org/10.1155/2024/8222314.
[128] H. Vasylyeva, I. Mironyuk, I. Mykytyn, *Structural, morphological, and adsorption properties of titanium dioxide doped with Fluorine,* Physics and Chemistry of Solid State, 26(2), 267 (2025); https://doi.org/10.15330/pcss.26.2.267-276.
[129] H. Vasylyeva, et el., *Adsorption of barium and zinc ions by mesoporous TiO_2 with chemosorbed carbonate groups,* Physics and Chemistry of Solid State, 20(3), 282 (2019); https://doi.org/10.15330/pcss.20.3.282-290.
[130] H. Dehouli, et el., *Influences of pH, temperature and activated carbon properties on the interaction ozone/activated carbon for a wastewater treatment process,* Desalination, 254(1–3), 12 (2010); https://doi.org/10.1016/j.desal.2009.12.021.
[131] H.-Y. Hong, et el., *Ultrasonic regeneration studies on activated carbon loaded with isopropyl alcohol,* Applied Sciences, 10(21), 7596 (2020); https://doi.org/10.3390/app10217596.
[132] Ü. Geçgel, O. Üner, *Adsorption of bovine serum albumin onto activated carbon prepared from Elaeagnus stone*, Bulletin of the Chemical Society of Ethiopia, 32(1), 53 (2018); https://doi.org/10.4314/bcse.v32i1.5.
[133] J. J. M. Orfão, et el., *Adsorption of a reactive dye on chemically modified activated carbons—Influence of pH*, Journal of Colloid and Interface Science, 296(2), 480 (2006); https://doi.org/10.1016/j.jcis.2005.09.063.
[134] T. J. M. Fraga, et el., *Amino-Fe_3O_4-functionalized graphene oxide as a novel adsorbent of Methylene Blue: kinetics, equilibrium, and recyclability aspect,* Environmental Science and Pollution Research, 26(28), 28593 (2019); https://doi.org/10.1007/s11356-018-3139-z.
[135] M. A. El-Nemr, et el., *Modelling of a new form of nitrogen doped activated carbon for adsorption of various dyes and hexavalent chromium ions,* Scientific Reports, 15(1), 3896 (2025); https://doi.org/10.1038/s41598-025-87398-6.

[136] M. Heidarizad, S.S. Şengör, *Synthesis of graphene oxide/magnesium oxide nanocomposites with high-rate adsorption of methylene blue,* Journal of Molecular Liquids, 224, 607 (2016); https://doi.org/10.1016/j.molliq.2016.09.049.
[137] M. T. Stone, M. Kozlov, *Separating proteins with activated carbon,* Langmuir, 30(27), 8046 (2014); https://doi.org/10.1021/la501005s.
[138] M. Sultana, et el., *A review on experimental chemically modified activated carbon to enhance dye and heavy metals adsorption* 6, Cleaner Engineering and Technology, 100382 (2022); https://doi.org/10.1016/j.clet.2021.100382.
[139] T. J. Bandosz, C. O. Ania, Interface Science and Technology, Chapter 4 Surface chemistry of activated carbons and its characterization (Elsevier, 2006); https://doi.org/10.1016/S1573-4285(06)80013-X.
[140] J. A. Menéndez-Díaz, I. Martín-Gullón, Chapter 1 Types of carbon adsorbents and their production (Elsevier, 2006); https://doi.org/10.1016/S1573-4285(06)80010-4.
[141] D. Berillo, A. Ermukhambetova, *The review of oral adsorbents and their properties,* Adsorption: Journal of the International Adsorption Society, 30(6), 1505 (2024); https://doi.org/10.1007/s10450-024-00515-1.
[142] Y. Zhang, et el., *Interactions of graphene and graphene oxide with proteins and peptides*, Nanotechnology Reviews, 2(1), 27 (2013); https://doi.org/10.1515/ntrev-2012-0078.
[143] M. Andayani, et el., *Development of graphene and graphene quantum dots toward biomedical engineering applications: A review,* Nanotechnology Reviews, 12(1), 20230168 (2023); https://doi.org/10.1515/ntrev-2023-0168,
[144] F. Ahmad, et el., *Graphene and its derivatives in medical applications: A comprehensive review,* Synthetic Metals, 304, 117594 (2024); https://doi.org/10.1016/j.synthmet.2024.117594,
[145] A. Gostaviceanu, et el., *Graphene-oxide peptide-containing materials for biomedical applications*, International Journal of Molecular Sciences, 25(18), 10174 (2024); https://doi.org/10.3390/ijms251810174.
[146] I. Mironyuk, et el., *Structural-morphological and adsorption properties of hollow balls of oxidized graphene obtained by auto-combustion of saccharose,* Nano-Structures & Nano-Objects, 41, 101462 (2025); https://doi.org/10.1016/j.nanoso.2025.101462.
[147] K. Tadyszak, J. K. Wychowaniec, J. Litowczenko, B*iomedical applications of graphene-based structures*, Nanomaterials, 8(11), 944 (2018); https://doi.org/10.3390/nano8110944.
[148] N. S. Ekal, et el., *Oxidation state of graphene oxide nanosheets drives their interaction with proteins: A case of bovine serum albumin,* Colloids and Surfaces B: Biointerfaces, 212, 112367 (2022); https://doi.org/10.1016/j.colsurfb.2022.112367.
[149] N. Bellier, et el., *Recent biomedical advancements in graphene oxide- and reduced graphene oxide-based nanocomposite nanocarriers,* Biomaterials Research, 26(1), 65 (2022); https://doi.org/10.1186/s40824-022-00313-2.
[150] R. Kumar, et el., *Graphene-based materials for biotechnological and biomedical applications: Drug delivery, bioimaging and biosensing,* Materials Today: Chemistry, 33, 101750 (2023); https://doi.org/10.1016/j.mtchem.2023.101750.
[151] Z. U. N. Mughal, et el., *Determination of vitamins K1, K2, B6, and D3 using reduced graphene oxide fabricated using a bismuth nanoparticle embedded polypyrrole nanocomposite based optical sensor,* Materials Advances, (2024); https://doi.org/10.1039/D3MA01149F.
[152] R. Kumar, et el., *Effect of band gap of graphene oxide on interaction with bovine serum albumin: Correlation of band gap with sensitivity,* Carbon Trends, 15(100367), 100367 (2024); https://doi.org/10.1016/j.cartre.2024.100367.
[153] A. Vasilescu, et el., *Porous reduced graphene oxide modified electrodes for the analysis of protein aggregation. Part 1: Lysozyme aggregation at pH 2 and 7.4,* Electrochimica Acta, 254, 375 (2017); https://doi.org/10.1016/j.electacta.2017.09.083.
[154] H. Zhang, et el., *Changing the activities and structures of bovine serum albumin bound to graphene oxide,* Applied Surface Science, 427, 1019 (2018); https://doi.org/10.1016/j.apsusc.2017.08.130.
[155] B. Sun, et el., *New insights into the colloidal stability of graphene oxide in aquatic environment: Interplays of photoaging and proteins,* Water Research, 200, 117213 (2021); https://doi.org/10.1016/j.watres.2021.117213.
[156] Y. Yang, et el., *Protein corona reduced graphene oxide cytotoxicity by inhibiting endocytosis,* Colloids and Interface Science Communications, 45, 100514 (2021); https://doi.org/10.1016/j.colcom.2021.100514.
[157] W. Nakanishi, et el., *Bioactive nanocarbon assemblies: Nanoarchitectonics and applications,* Nano Today, 9(3), 378 (2014); https://doi.org/10.1016/j.nantod.2014.05.002.
[158] B. Nagy, et el., *Double probe approach to protein adsorption on porous carbon surfaces,* Carbon, 112, 103 (2016); https://doi.org/10.1016/j.carbon.2016.10.095.
[159] K. Imamura, et el., *Adsorption characteristics of various proteins to a titanium surface,* Journal of Bioscience and Bioengineering, 106(3), 273 (2008); https://doi.org/10.1263/jbb.106.273.
[160] A. M. Puziy, et el., *Kinetics of protein adsorption by nanoporous carbons with different pore size,* Adsorption: Journal of the International Adsorption Society, 22(4–6), 541 (2016); https://doi.org/10.1007/s10450-015-9723-3.
[161] P.A. Fritz, et el., *Electrode surface potential-driven protein adsorption and desorption through modulation of electrostatic, van der Waals* and hydration interactions, Langmuir: The ACS Journal of Surfaces and Colloids, 37(21), 6549 (2021); https://doi.org/10.1021/acs.langmuir.1c00828.
[162] K. C. Dee, D. A. Puleo, R. Bizios, Chapter 3 Protein-surface interactions, in An Introduction to Tissue-Biomaterial Interactions (John Wiley & Sons, Inc., New York, 2002); https://doi.org/10.1002/0471270598.ch3,
[163] S. P. Mitra, *Protein adsorption on biomaterial surfaces: Subsequent conformational and biological consequences – A review,* Journal of Surface Science and Technology, 36(1–2), 7 (2020); https://doi.org/10.18311/jsst/2020/23282

[164] Y. L. Jeyachandran, et el., *Efficiency of blocking of non-specific interaction of different proteins by BSA adsorbed on hydrophobic and hydrophilic surfaces,* Journal of Colloid and Interface Science, 341(1), 136 (2010); https://doi.org/10.1016/j.jcis.2009.09.007.
[165] R. A. Latour, *Fundamental principles of the thermodynamics and kinetics of protein adsorption to material surfaces,* Colloids and Surfaces B: Biointerfaces, 191, 110992 (2020); https://doi.org/10.1016/j.colsurfb.2020.110992.
[166] P. Rajasekar, et el., *Interaction of BSA with graphene oxide: Influence on the bioactivity of graphene oxide,* Diamond and Related Materials, 132, 109629 (2023); https://doi.org/10.1016/j.diamond.2022.109629,
[167] C. F. Wertz, M. M. Santore, *Adsorption and reorientation kinetics of lysozyme on hydrophobic surfaces,* Langmuir: The ACS Journal of Surfaces and Colloids, 18(4), 1190 (2002); https://doi.org/10.1021/la0108813.
[168] G. J. Ma, et el., *Understanding how natural sequence variation in serum albumin proteins affects conformational stability and protein adsorption,* Colloids and Surfaces B: Biointerfaces, 194, 111194 (2020); https://doi.org/10.1016/j.colsurfb.2020.111194.
[169] A. Sonoi, I. Furikado, K. Ishihara, *Effects of initially adsorbed proteins on substrate surfaces during multilayer heterogeneous protein adsorption*, Langmuir: The ACS Journal of Surfaces and Colloids, 37(13), 3897 (2021); https://doi.org/10.1021/acs.langmuir.1c00091.
[170] T. Arai, W. Norde, *The behavior of some model proteins at solid-liquid interfaces 1. Adsorption from single protein solutions,* Colloids and Surfaces, 51, 1 (1990); https://doi.org/10.1016/0166-6622(90)80127-P.
[171] J. Lyklema, W. Norde, *Interfacial behaviour of biomacromolecules,* Progress in Colloid and Polymer Science, 9 (2007); https://doi.org/10.1007/BFb0114438.
[172] J. Koo, et el., *Pressure-induced protein adsorption at aqueous-solid interfaces,* Langmuir, 29 (25), 8025 (2013); https://doi.org/10.1021/la401296f.
[173] K. Bozgeyik, T. Kopac, *Adsorption Properties of Arc Produced Multi-Walled Carbon Nanotubes for Bovine Serum Albumin,* International Journal of Chemical Reactor Engineering, 14(2), 549 (2016); https://doi.org/10.1515/ijcre-2015-0160.
[174] K. Bozgeyik, T. Kopac, *Synthesis of multi-walled carbon nanotube-zirconia composite and bovine serum albumin adsorption characteristics,* Materials Science Forum, 900, (2017); https://doi.org/10.4028/www.scientific.net/MSF.900.27.
[175] T. Kopac, K. Bozgeyik, E. Flahaut, *Adsorption and interactions of the bovine serum albumin–double walled carbon nanotube system,* Journal of Molecular Liquids, 252, 1 (2018); https://doi.org/10.1016/j.molliq.2017.12.100
[176] Y. Huang, et el., *Protein adsorption behavior on reduced graphene oxide and boron-doped diamond investigated by electrochemical impedance spectroscopy,* Carbon, 152, 354 (2019); https://doi.org/10.1016/j.carbon.2019.06.023.

Ірина Прокіпчук[1], Іван Миронюк[1], Ігор Микитин[1], Ганна Васильєва[2]

Адсорбція білків на вуглецевих матеріалах. Огляд

[1]Кафедра хімії, Карпатський національний університет імені Василя Стефаника, Івано-Франківськ, Україна,
iryna.prokipchuk@pnu.edu.ua
[2]Відділ радіаційної безпеки, ДВНЗ «Ужгородський національний університет», Ужгород, Україна,
h.v.vasylyeva@hotmail.com

Адсорбція білків на вуглецевих матеріалах є складним і багатогранним процесом, який має вирішальне значення для застосування в біотехнології, медицині, екології та матеріалознавстві. У цьому огляді всебічно розглядаються фізико-хімічні механізми, що визначають адсорбцію білків на різних вуглецевих матеріалах, включаючи активоване вугілля, графен і оксид графену. Акцент зроблено на властивостях поверхні, таких як пористість, хімічний склад поверхні, змочуваність та електричний заряд, а також на характеристиках білків, зокрема їхньому розмірі, структурі, заряді та конформаційній динаміці. Розглянуто вплив факторів середовища – pH, іонної сили та концентрації білка – на поведінку адсорбції та формування білкового шару. Особлива увага приділяється ролі кисневмісних функціональних груп на поверхнях вуглецю та їх впливу на електростатичні та водневі взаємодії. Також надається огляд аналітичних методів, що використовуються для вивчення адсорбції, включаючи атомно-силову мікроскопію (АСМ), круговий дихроїзм (КД), ізотермічну титраційну калориметрію (ІТК), кварцовий кристалічний мікробаланс (ККМ) та спектроскопічні методи. В огляді описано роль адсорбції білків на вуглецевих матеріалах для їх біомедичних застосувань, а саме для підвищення біосумісності імплантатів та розробки біосенсорів. Також підкреслено стрімке зростання кількості робіт, присвячених дослідженню сорбції на оксиді графену в останні роки, а також зростаючий інтерес до його використання для розробки сенсорів.

Ключові слова: адсорбція, графен, оксид графену, активоване вугілля, вуглецеві сорбенти, теоретичні моделі.